

# Pigment signatures of phytoplankton communities in the Beaufort Sea

P. Coupel<sup>1</sup>, A. Matsuoka<sup>1</sup>, D. Ruiz-Pino<sup>2</sup>, M. Gosselin<sup>3</sup>, D. Marie<sup>4</sup>, J.-É. Tremblay<sup>1</sup>, and M. Babin<sup>1</sup>

<sup>1</sup>Joint International ULaval-CNRS Laboratory Takuvik, Québec-Océan, Département de Biologie, Université Laval, Québec, Québec G1V 0A6, Canada

<sup>2</sup>Laboratoire d'Océanographie et du Climat: Expérimentation et Approches Numériques (LOCEAN), UPMC, CNRS, UMR 7159, Paris, France

<sup>3</sup>Institut des sciences de la mer de Rimouski (ISMER), Université du Québec à Rimouski, 310 allée des Ursulines, Rimouski, Québec, G5L 3A1, Canada

<sup>4</sup>Station Biologique, CNRS, UMR 7144, INSU et Université Pierre et Marie Curie, Place George Teissier, 29680 Roscoff, France

Correspondence to: P. Coupel (Pierre.Coupel@takuvik.ulaval.ca)

**Abstract.** Phytoplankton are expected to respond to recent environmental changes of the Arctic Ocean. In terms of bottom-up control, modifying the phytoplankton distribution will ultimately affect the entire food web and carbon export. However, detecting and quantifying change in phytoplankton communities in the Arctic Ocean remains difficult because of the lack of data and the inconsistent identification methods used. Based on pigment and microscopy data sampled in the Beaufort Sea during summer 2009, we optimized the chemotaxonomic tool CHEMTAX for the assessment of phytoplankton community composition in an Arctic setting. The geographical distribution of the main phytoplankton groups was determined with clustering methods. Four phytoplankton assemblages were determined and related to bathymetry, nutrients and light availability. Surface waters across the whole survey region were dominated by prasinophytes and chlorophytes, whereas the subsurface chlorophyll maximum was dominated by the centric diatoms *Chaetoceros socialis* on the shelf and by two populations of nanoflagellates in the deep basin. Microscopic counts showed a high contribution of the heterotrophic dinoflagellates *Gymnodinium* and *Gyrodinium* spp. to total carbon biomass, suggesting high grazing activity at this time of the year. However, CHEMTAX was unable to detect these dinoflagellates because they lack peridinin. The inclusion in heterotrophic dinoflagellates of the pigments of their prey potentially leads to incorrect group assignments and some misinterpretation of CHEMTAX. Thanks to the high reproducibility of pigment analysis, our results can serve as a baseline to assess change and spatial or temporal variability in several phytoplankton populations that are not affected by these misinterpretations.

## 1. Introduction

The Arctic environment is undergoing transformations caused by climate change highlighted by the accelerating reduction of the summer sea ice extent (Comiso et al., 2008; Rothrock et al., 1999; Stroeve et al., 2011). Rapid response of phytoplankton diversity and dominance has already been discussed (Carmack and Wassmann, 2006). A shift towards smaller phytoplankton was suggested in the Canadian Arctic as a result of low nitrate availability and strong stratification (Li et al., 2009). A recent study suggested that

44 nanoflagellates would be promoted in the newly ice-free basins as a consequence of the  
45 deepening nitracline (Coupel et al., 2012). More frequent wind-driven upwelling events could  
46 multiply the production and favour the development of large taxa such as diatoms (Pickart et  
47 al., 2013; Tremblay et al., 2011). The earlier ice retreat may affect the zooplankton and  
48 benthos by altering the timing and location of the spring bloom and associated species  
49 succession (Grebmeier et al., 2010; Hunt Jr et al., 2002). In response to these changes, a  
50 reorganization of the Arctic Ocean food web would be expected causing changes in the  
51 function of the ecosystem and ultimately fisheries but also on biogeochemical cycles  
52 (Falkowski, 2000) and carbon export (Sigman and Boyle, 2000; Wassmann and Reigstad,  
53 2011).

54 Monitoring the diversity and dominance of Arctic phytoplankton is a prerequisite to  
55 document change. However, it is very difficult to detect responses of phytoplankton in the  
56 Arctic due to a lack of quantitative information on taxonomic composition (Poulin et al.,  
57 2010; Wassmann et al., 2011). The various approaches used for phytoplankton identification  
58 greatly increased the breadth of knowledge on phytoplankton communities but limit the  
59 possibility of inter-comparisons between different datasets. In the aim to detect year-to-year  
60 main changes in the phytoplankton communities a reproducible method needs to be  
61 established. Optical microscopy is a good method to identify and enumerate large  
62 phytoplankton and also to deduce the carbon biomass of phytoplankton but the procedure is  
63 expensive, time-consuming and relies greatly on the skill of the taxonomist (Wright and  
64 Jeffrey, 2006). Flow cytometry and molecular analyses are better suited to identify small  
65 phytoplankton (Ansotegui et al., 2001; Roy et al., 1996; Schlüter et al., 2000). The remote  
66 sensing approach is becoming increasingly attractive with the recent advances in the  
67 interpretation of optical signals to detect diatoms and other phytoplankton groups from space  
68 (Alvain et al., 2005; Hirata et al., 2011; Sathyendranath et al., 2004; Uitz et al., 2006). But  
69 these approaches, developed with in-situ dataset from non-polar regions, still need to be  
70 adapted and tuned for the Arctic region. Moreover, the satellite method is restricted to the  
71 surface layer and is still limited by the presence of sea ice, frequent cloudy conditions and  
72 coastal turbidity in the Arctic Ocean (IOCCG 2014).

73 The use of pigments as markers of major phytoplankton groups is a good candidate to  
74 monitor dominant phytoplankton groups although being limited by the acquisition of water  
75 samples during oceanographic cruises. Automated measurements of pigment concentrations  
76 using high performance liquid chromatography (HPLC) allows fast and highly reproducible  
77 analyses (Jeffrey et al., 1997). Moreover, pigment analysis allows for the characterization of  
78 both the large and small size phytoplankton (Hooker et al., 2005). The main issue when using  
79 pigments for quantitative taxonomy is the overlap of several pigments among phytoplankton  
80 groups. The chemotaxonomic software CHEMTAX was developed to overcome this problem  
81 by considering a large suite of pigments simultaneously (Mackey et al., 1996). CHEMTAX  
82 has been widely used in the global ocean, notably in Antarctic polar waters (Kozłowski et al.,  
83 2011; Rodriguez et al., 2002; Wright et al., 1996).

84 Few studies have used CHEMTAX in the Arctic Ocean to date. Spatial and temporal  
85 variability of the phytoplankton community structure were described for the North Water  
86 Polynya (Vidussi et al., 2004) and the Canada Basin (Coupel et al., 2012; Taylor et al., 2013),  
87 while Alou-Font et al. (2013) used CHEMTAX to describe the influence of snow conditions  
88 on the sea-ice communities of Amundsen Gulf. Phytoplankton communities were also  
89 investigated using CHEMTAX in subarctic regions, i.e. the Bering Sea (Suzuki et al., 2002)  
90 and in the Faroe-Shetland channel (Riegman and Kraay, 2001). Investigations of the  
91 reliability of CHEMTAX underscores the need to adapt procedures to the targeted area by  
92 investigating the dominant species, their pigment content and the environmental conditions  
93 such as light availability and nutrient status (Wright and Jeffrey, 2006). Despite this caveat

94 most prior studies using CHEMTAX in the Arctic Ocean have used a parameterization made  
95 for Antarctic waters. Inappropriate parameterization of CHEMTAX has been identified as the  
96 main source of misinterpretation in taxonomic determinations based on pigments (Irigoiien et  
97 al., 2004; Lewitus et al., 2005). Knowing this, a regional parameterization of CHEMTAX is  
98 required before using it to examine possible changes in the phytoplankton community  
99 structure. Then, regional settings could be used as starting point for other Arctic CHEMTAX  
100 work.

101 The objective of this study was to examine Arctic phytoplankton community structure by  
102 CHEMTAX using samples collected during summer in the Beaufort Sea. This region, which  
103 is influenced by freshwater from the Mackenzie River over the narrow continental shelf and  
104 by oceanic waters and ice-melt waters in the deep ocean basin, allowed us to test the  
105 performance of CHEMTAX under diverse environmental conditions. Accurate taxonomic  
106 identification and enumeration of cells  $> 3\mu\text{m}$  were combined with flow-cytometric sorting  
107 and counting of picophytoplankton cells (1-3  $\mu\text{m}$ ) to identify the dominant phytoplankton  
108 groups. The pigment ratios of these dominant Arctic groups were then found in the literature  
109 and used to tune the CHEMTAX software for the Beaufort Sea region. This work  
110 demonstrates the use of CHEMTAX to describe phytoplankton populations, and similar  
111 studies conducted in the future could be used to investigate changes in populations over time.

## 112 2. Materials and methods

113 Hydrographical observations and seawater sampling were carried out in the Beaufort Sea  
114 ( $69^{\circ}$ - $73^{\circ}\text{N}$ ;  $125$ - $145^{\circ}\text{W}$ ) during Leg 2b of the MALINA cruise in summer 2009 (30 July to  
115 27 August 2009) onboard the CCGS *Amundsen*. Twenty stations were sampled on the  
116 Mackenzie shelf and the deep waters of the Beaufort Sea (Fig. 1) using Niskin-type bottles  
117 mounted on a CTD-Rosette system equipped with sensors to measure photosynthetically  
118 active radiation (PAR; Biospherical QCP-2300), temperature and salinity (Sea-Bird SBE-  
119 911plus). Phytoplankton communities were investigated using three different approaches:  
120 pigment signature (386 samples), light microscopy (88 samples) and flow cytometry (182  
121 samples).

### 122 2.1. Pigments

123 We followed the HPLC analytical procedure proposed by Van Heukelem and Thomas  
124 (2001). Briefly, photosynthetic phytoplankton pigments were sampled at 6 to 10 depths in the  
125 upper 200 m of the water column, however only samples from the surface (5m) and sub-  
126 surface chlorophyll *a* maximum (SCM) are presented in this work. Seawater aliquots ranging  
127 from 0.25 to 2.27 litres were filtered through 25 mm Whatman GF/F filters (nominal pore size  
128 of 0.7  $\mu\text{m}$ ) and frozen immediately at  $-80^{\circ}\text{C}$  in liquid nitrogen until the analysis. Analyses  
129 were performed at the Laboratoire d'Océanographie de Villefranche (LOV). Filters were  
130 extracted in 3 mL methanol (100%) for 2 hours, disrupted by sonication, centrifuged and  
131 filtered (Whatman GF/F). The extracts were injected within 24 hours onto a reversed phase  
132 C8 Zorbax Eclipse column (dimension:  $3 \times 150$  mm,  $3.5\mu\text{m}$  pore size). Instrumentation  
133 comprised an Agilent Technologies 1100 series HPLC system with diode array detection at  
134 450 nm (carotenoids and chlorophylls *c* and *b*), 676 nm (chlorophyll *a* and derivatives), and  
135 770 nm (bacteriochlorophyll *a*). The concentrations of 21 pigments, including the  
136 chlorophyll *a* (Chl *a*), were obtained and used in this study (see Table 1 for details and  
137 pigment abbreviations). The limits of detection ( $3 \times$  noise) for the different pigments, based  
138 on a filtered volume of 2 L ranged from 0.0001 to  $0.0006 \text{ mg m}^{-3}$ . The precision of the  
139 instrument was tested using injected standards and showed a variation coefficient of 0.35%.  
140 Moreover, previous tests of the precision of the instrument and method used here were

141 conducted on field samples replicates. A coefficient of variation of 3.2% and 4% was found  
142 for the primary and secondary pigment, respectively. Such precision was in accordance with  
143 the 3% standard high precision required in the analysis of field samples (Hooker et al., 2005).

## 144 2.2. Light microscopy and flow cytometry

145 One to six depths were sampled in the upper 100 m of the water column for taxonomic  
146 identification and enumeration of phytoplankton cells by light microscopy. Samples were  
147 preserved in acidic Lugol's solution and stored in the dark at 4°C until analysis. The counting  
148 of cells > 3 µm was performed using an inverted microscope (Wild Heerbrugg and Zeiss  
149 Axiovert 10) following the Utermöhl method with settling columns of 25 mL and 50 mL  
150 (Lund et al., 1958). A minimum of 400 cells were counted over at least 3 transects.  
151 Autotrophic and heterotrophic protists were counted. The autotrophic phytoplankton were  
152 distributed among 10 classes plus a group of unidentified flagellates (Table 2). Unidentified  
153 cells (> 3 µm) represented less than 10% of the total cell abundance over the shelf but reached  
154 75% of the total cell abundance over the basin. Half of the unidentified cells were < 5 µm.  
155 Enumeration of picophytoplankton (1-3µm) by flow cytometry analysis (Marie et al., 1997)  
156 was performed onboard using a FACSaria (Becton Dickinson, San Jose, CA, USA) and  
157 following the method described in Balzano et al. (2012).

## 158 2.3. Converting abundance to carbon biomass

159 Phytoplankton abundances obtained by light microscopy and flow cytometry were converted  
160 into carbon biomass (Table 2). The carbon biomass ( $C$ , ng C m<sup>-3</sup>) is obtained by multiplying  
161 cell abundance ( $A$ , cells L<sup>-1</sup>) by mean cellular carbon content ( $CC$ , ng C cell<sup>-1</sup>) for each  
162 phytoplankton group:

$$164 C = A \times CC,$$

165 where  $CC$  was derived from cell biovolume  $BV$  (µm<sup>3</sup>) using three conversion equations  
166 determined by regression analysis on a large dataset (Menden-Deuer and Lessard, 2000).  
167 Diatoms and dinoflagellates require particular formulas because of their low (diatoms) or high  
168 (dinoflagellates) specific carbon content relative to other protists:

$$171 \text{ Diatoms: } CC = 0.288 \times BV^{0.811}$$

$$172 \text{ Dinoflagellates: } CC = 0.760 \times BV^{0.819}$$

$$173 \text{ All other protists (except diatoms and dinoflagellates): } CC = 0.216 \times BV^{0.939},$$

174 where species  $BV$  were compiled from Olenina et al. (2006). When species  $BV$  were not  
175 referenced, biovolumes were estimated according to cell shape and dimensions (Bérard-  
176 Therriault et al., 1999) using appropriate geometric formulas (Olenina et al., 2006). Replicate  
177 measurements of the diameter of some common diatom and dinoflagellate species shows  
178 variability in the biovolume around 30% (Menden-Deuer and Lessard, 2000; Olenina et al.,  
179 2006). A 30% overestimation of the biovolume of a species would cause a 20 to 30%  
180 overestimation of its carbon biomass depending on the conversion equation used.

181 According to the three conversion equations, a large sized dinoflagellate ( $BV = 10000 \mu\text{m}^3$ )  
182 contains 3 times more carbon than a diatom of the same biovolume and 15% more carbon  
183 than a protist of the same biovolume. However, in the case of a small cell volume ( $BV = 10$   
184  $\mu\text{m}^3$ ), a dinoflagellate would contain 2.5 times more carbon than both a diatom and a protist.

185

#### 186 2.4. Pigment interpretation: CHEMTAX

187 The CHEMTAX method (Mackey et al., 1996) was used to estimate the algal class  
188 biomass from measurements of *in situ* pigment. Two **inputs** are required to create the **ratio**  
189 **matrix** used to run the CHEMTAX program: the major phytoplankton groups present in our  
190 study area (chemotaxonomic classes) and their pigment content expressed as initial  
191 « pigment/TChl *a* » ratios where TChl *a* is the total Chl *a* concentration, i.e. the sum of Chl *a*  
192 and **chlorophyllide *a* (Chlide *a*)**, Table 3A).

193 The algal groups identified by microscopy were grouped in 9 chemotaxonomic classes. The  
194 very high dominance of the centric diatom *Chaetoceros socialis* in several stations over the  
195 shelf allowed **us** to accurately define the pigment/TChl *a* ratios of the diatom class. For the  
196 other phytoplankton groups, **due to the fact that** their specific pigment signatures were always  
197 mixed with other group signatures, we used the pigment/TChl *a* ratios from the literature.  
198 Then, we chose the ratios representative of the dominant species associated with each  
199 chemotaxonomic class previously identified with microscopy. The dinoflagellate class  
200 represents the dinoflagellates containing **peridinin (Peri)** as *Heterocapsa rotundata* whose  
201 ratio Peri/TChl *a* was set to 0.6 (Vidussi et al., 2004). The *c*<sub>3</sub>-flagellates group corresponds to  
202 the Dino-2 class defined in Higgins et al. (2011) which included the dinoflagellates type 2  
203 lacking pigment Peri. We chose here to replace the group name Dino-2 by *c*<sub>3</sub>-flagellates  
204 because we think the characteristics of this groups, i.e. a relatively high **chlorophyll *c*<sub>3</sub> (Chl**  
205 ***c*<sub>3</sub>)** concentration relative to their **19'-butanoyloxyfucoxanthin (But-fuco)** and **19'-**  
206 **hexanoyloxyfucoxanthin (Hex-fuco)** concentrations, included a larger diversity of flagellates  
207 including raphidophytes **and** dictyochophytes in addition to the autotrophic dinoflagellates  
208 lacking Peri. The cryptophytes were detected by the presence of **alloxanthin (Allo)** pigment.  
209 The haptophytes type 7 class refers to the prymnesiophytes type *Chrysochromulina* spp.  
210 discriminated by a high ratio of Hex-fuco to TChl *a*. In contrast, the chrysophytes and  
211 pelagophytes contained a high ratio of But-fuco to TChl *a*. Finally, three groups of green  
212 algae containing **chlorophyll *b* (Chl *b*)** were considered: the chlorophytes, the prasinophytes  
213 type 2 and the prasinophytes type 3. The prasinophytes type 3 containing the pigment  
214 **prasinoxanthin (Pras)** is representative of the pico-sized species *Micromonas* sp. while the  
215 type 2 is associated with prasinophytes lacking Pras as the nano-sized *Pyramimonas* sp. The  
216 chlorophytes were evidenced by significant concentrations of **lutein (Lut)**, a characteristic  
217 pigment of this group (Del Campo et al., 2000). The effect of light levels on pigment ratios  
218 was taken into account by considering two **ratio matrices**, a high light **ratio matrix** runs on  
219 surface samples (0-20m) and low light **ratio matrix** runs on subsurface samples (20-200m).  
220 Moreover, photoprotective carotenoids (PPC = **diadinoxanthin (Diadino) + diatoxanthin**  
221 **(Diato) + zeaxanthin (Zea) + violaxanthin (Viola) + carotenes (Car)**) were not used since they  
222 varied strongly with irradiance and/or they are taxonomically widespread (Demers et al.,  
223 1991). Finally, we carried out independent CHEMTAX runs for shelf and basin samples to  
224 minimize the effects of the growth and nutrient conditions on the pigment interpretation.

225 The **ratio of pigment/Chl *a*** for various algal taxa used as « seed » values for the CHEMTAX  
226 analysis were chosen from the literature. However, the pigment ratios for a real sample are  
227 unlikely to be known exactly due to regional variations of individual species, strain  
228 differences within a given species and local changes in algal physiology due to environmental  
229 factors such as temperature, salinity, light field, nutrient stress and mixing regimes (Mackey  
230 et al., 1996). Therefore, to test the sensitivity of CHEMTAX, ten further high light and low  
231 light pigment ratio tables were generated by multiplying each cell of our initial **ratio matrix** by  
232 a randomly determined factor F, where  $F = 1 + S * (R - 0.5)$ . S is a scaling factor (normally  
233 0.7), and R is a random number between 0 and 1 generated using the Microsoft Excel RAND  
234 function. The random **ratio matrices** were created using a template provided by Thomas  
235 Wright (CSIRO, Australia). For the shelf and basin subset, each of the ten low light and high

236 light ratio tables were used as the starting point for a CHEMTAX optimization using iteration  
237 and a steepest descent algorithm to find a minimum residual. The solution with the smallest  
238 residual (final ratio matrix, Table 3B) was used to estimate the abundance of the  
239 phytoplankton classes, i.e. the part of the total Chl *a* associated with each phytoplankton class.  
240 The results of the ten matrices were used to calculate the average and standard deviation of  
241 the abundance estimates.

### 242 3. Results and discussion

243

244

#### 3.1. Spatial distribution of accessory pigments

245 The distribution of TChl *a* showed large horizontal and vertical variability in the Beaufort  
246 Sea in August 2009. A subsurface chlorophyll *a* maximum (SCM) was generally present both  
247 over the shelf ( $35 \pm 8$  m) and deep waters of the Beaufort Sea ( $61 \pm 7$  m). Surface TChl *a* was  
248 twice as high on the shelf ( $0.20 \pm 0.13$  mg Chl *a* m<sup>-3</sup>, Fig. 2a) than in the basins (Fig. 2c) and  
249 SCM TChl *a* was 10 times higher over the shelf ( $2.84 \pm 2.55$  mg Chl *a* m<sup>-3</sup>, Fig. 2b) than in  
250 the basins (Fig. 2d). The highest chlorophyll biomasses ( $> 6$  mg Chl *a* m<sup>-3</sup>) were observed at  
251 the SCM close to the shelf break (St 260 and 780, Fig. 1, 2b). Such high values contrast with  
252 the low ones ( $< 1$  mg Chl *a* m<sup>-3</sup>) observed during autumn in the same area in 2002 and 2003  
253 (Brugel et al., 2009).

254 The concentrations of accessory pigments also varied significantly across shelf and basin  
255 stations and between the surface and the SCM. The highest biomasses, observed at the SCM  
256 of shelf waters, were associated with the dominance of fucoxanthin (Fuco) and chlorophyll  
257 *c*<sub>1+2</sub> (Chl *c*<sub>1+2</sub>). These two pigments, characteristic of diatoms, represented 56% and 23% of  
258 the total accessory pigments biomass, respectively (Fig. 2b). The presence of degradation  
259 pigments of Chl *a* at the SCM of the shelf (Chlide *a* + pheophorbide *a* (Pheide *a*) +  
260 pheophytin *a* (Phe *a*) = 14% of total accessory pigments) indicated the presence of  
261 zooplankton fecal pellets or cellular senescence (Bidigare et al., 1986). The remaining 7%  
262 were mainly associated with photoprotective carotenoids (Diadino + Diato + Zea + Viola +  
263 Car = 6.7% of total accessory pigments).

264 In surface waters of the shelf (Fig. 2a), pigment assemblages were indicative of diverse  
265 communities consisting of diatoms, dinoflagellates, cryptophytes, prymnesiophytes and green  
266 algae. The contribution of Fuco (34% of total accessory pigments), Chl *c*<sub>1+2</sub> (13% of total  
267 accessory pigments) and degradation products of Chl *a* (9.7%) decreased while the proportion  
268 of Chl *b* to total accessory pigments increased from 0.3% at the SCM to 9% at the surface.  
269 Peri and Allo, reflecting dinoflagellates and cryptophytes, were observed at stations 394 and  
270 680 but remained poorly represented otherwise. The high contribution of photoprotective  
271 carotenoids to total accessory pigments (16.1%), compared to surface waters (6.7%),  
272 indicated the response of phytoplankton to high light (Frank et al., 1994; Fujiki and Taguchi,  
273 2002).

274 In the basin, pigments associated with green algae (Chl *b*, Pras, neoxanthin (Neo), Viola,  
275 Lut) and nanoflagellates (Hex-fuco, But-fuco, Chl *c*<sub>3</sub>) increased while diatom pigments  
276 decreased, i.e. Fuco and Chl *c*<sub>1+2</sub> (Fig. 2c,d). The highest contribution of nanoflagellate  
277 pigments Hex-fuco (18%), But-fuco (9%) and Chl *c*<sub>3</sub> (9%) were observed at the SCM. In  
278 contrast, the contribution of the green algal pigments Chl *b* (23%), Viola (5.9%) and Lut  
279 (4.3%), was higher at the surface than at the SCM. Degradation products represented less than  
280 3% of the total pigment load. Like on the shelf, the contribution of photoprotective  
281 carotenoids was three to four times higher at the surface ( $\approx 20\%$ ) than at the SCM (5.5%).

282 The few historical pigment data available for the Canadian Arctic show spatial  
283 patterns similar to those reported here. Hill et al. (2005) in the western Beaufort Sea and  
284 Coupel et al. (2012) in the Canada Basin and the Chukchi Sea agree on the dominance of

285 Fuco and Chl  $c_{1+c_2}$  over the shelf and an increase of pigments indicative of green algae (Pras,  
286 Chl  $b$ ) and nanoflagellates (Hex-fuco, But-fuco) offshore. However, some differences also  
287 exist, possibly reflecting the influence of distinct ice conditions on the phytoplankton  
288 assemblage. While in summer 2008 a high contribution of Fuco was found in the surface  
289 waters of the southern Canada basin free of ice (Coupel et al., 2012), Hill et al. (2005) in  
290 summer of 2002 in the same area but covered by ice, found lower Fuco and a greater  
291 contribution of Pras. Furthermore, the contribution of Pras at the SCM of basin stations was  
292 twice as high in 2008 than in 2002. Finally the pigments Hex-fuco and Chl  $c_3$ , characteristic  
293 of prymnesiophytes, contributed less in both 2002 and 2008 studies than in our 2009 data.

### 294 3.2. Phytoplankton group contribution

295 The surface and subsurface pigment assemblages shown in Fig. 2 were converted into  
296 relative contributions of main phytoplankton groups to TChl  $a$  with the CHEMTAX software.  
297 We first tested the sensitivity of the software by running CHEMTAX on our dataset using 5  
298 different ratio matrices from previous studies of polar oceans. The resulting CHEMTAX  
299 interpretation of the pigment assemblages varies widely according to the matrix used (Fig. 3).  
300 The diatom contribution to SCM assemblages at basin stations of the Beaufort Sea varied  
301 from 3.5% when using a parameterization for the North Polynya to 40% when using a  
302 parameterization for the Antarctic Peninsula. Similarly, the prasinophytes contribution ranged  
303 from 15% to 46% depending on the initial ratio matrix used. These differences arise from the  
304 different species and pigment/TChl  $a$  ratios used as “seed” values in CHEMTAX. Optimizing  
305 “seed” values for our study clearly requires an investigation of dominant species and their  
306 pigment content in the Beaufort Sea. Here we did this by first identifying the dominant  
307 phytoplankton species under optical microscopy (see section 2.4.). We tested the sensitivity of  
308 CHEMTAX by multiplying each number of the ratio matrix by a random factor. Our results  
309 show that by independently and randomly varying the ratios up to 35% of their initial values  
310 do not significantly modify the abundance estimates of the phytoplankton classes by  
311 CHEMTAX. The standard deviation in estimating the relative abundance of the  
312 phytoplankton classes ranged between 0.1% and 8% with an average deviation of 2%.  
313 Highest deviation was found for the Prasino-2 and Prasino-3 classes (about 5%) while the  
314 variation of the others groups were less than 2% on average. We suggest that changing the  
315 starting ratios by more or less a threshold value of 50% ensures confidence in the CHEMTAX  
316 output.

317 After running CHEMTAX on our dataset, the stations were classified with the  $k$ -means  
318 clustering method (MacQueen, 1967) according to their pigment resemblance/dissembance.  
319 Four significantly different phytoplankton communities were highlighted by the cluster  
320 classification (Fig. 4a). Cluster 1 was dominated at 95% by diatoms and represented the SCM  
321 of stations located on the shelf as well as surface waters close to Cap Bathurst and the  
322 Mackenzie estuary (Fig. 4b,c). Cluster 2 included surface waters of basin and shelf stations,  
323 characterized by a dominance of green algae (40%) shared between type 3 prasinophytes  
324 (25%) and chlorophytes (16%). Diatoms, dinoflagellates and cryptophytes were also major  
325 contributors of cluster 2 with 20%, 12% and 7% respectively. Clusters 3 and 4 were restricted  
326 to the SCM of basin stations and characterized by a high contribution of flagellates (Fig. 4a,  
327 c). Cluster 4 was dominated by prymnesiophytes (41%) while  $c_3$ -flagellates dominated cluster  
328 3 (28%). The contribution of green algae remained high in clusters 3 and 4 but was shared  
329 between prasinophytes of types 2 and 3 while chlorophytes were no longer present.

### 330 3.3. Linkages between phytoplankton assemblages and environmental factors

331 The four assemblages of phytoplankton inferred from pigments (Fig. 4a) were compared  
332 to environmental conditions (Table 4). Statistical analysis (Student’s test) showed significant

333 difference between the environmental conditions of the four clusters. The green algae,  
334 especially pico-sized prasinophytes of type 3, dominated the oligotrophic ( $0.12 \pm 0.13$  mg  
335 Chl *a* m<sup>-3</sup>) and nutrient-depleted surface waters (Cluster 2). This is consistent with the high  
336 surface/volume ratios of the picophytoplankton, which allows for more effective nutrient  
337 acquisition and better resistance to sinking. Dominance of the prasinophyte *Micromonas* sp.  
338 in the Beaufort Sea has been previously highlighted and especially under reduced sea ice  
339 cover (Comeau et al., 2011; Li et al., 2009; Lovejoy et al., 2007). Otherwise, the high  
340 Lut/Chl *b* ratio ( $\approx 0.2$ ) points out a significant contribution of chlorophytes in surface waters,  
341 a group including several freshwater species. The restriction of this group to the surface low  
342 salinity waters in our study makes us think the Mackenzie River could have spread them in  
343 the Beaufort Sea as previously proposed by Brugel et al. (2009). Finally, dinoflagellates  
344 identified in surface waters of cluster 2 have been previously underlined as a major  
345 contributor of the large autotrophic cells abundance on the Mackenzie shelf (Brugel et al.,  
346 2009).

347 The cluster 1 was sub-divided in two sub-clusters (cluster 1 surf and cluster 1 SCM,  
348 Table 4) because of the important environmental difference between surface and SCM. At the  
349 SCM of shelf stations (Cluster 1 SCM), nitrate concentrations were high ( $3.1 \pm 2.8$   $\mu\text{mol L}^{-1}$ )  
350 and possibly support substantial new production. The highest biomasses of the cruise ( $1.8 \pm$   
351  $2.3$  mg Chl *a* m<sup>-3</sup> and  $80 \pm 45$  mg C m<sup>-3</sup>) were measured in these waters and were related to a  
352 high dominance of diatoms. The diatom population could be fed by a cross-shelf flow of  
353 nitrate-rich waters from the basin to the shelf bottom (Carmack et al., 2004; Forest et al.,  
354 2014). The optical microscopy showed a strong dominance of the colonial centric diatoms  
355 *Chaetoceros socialis* ( $\approx 1 \times 10^9$  cell L<sup>-1</sup>, data not shown). This species is relatively small ( $\approx 10$   
356  $\mu\text{m}$ ) and often observed in succession to larger ones such as *Thalassiosira* spp. or  
357 *Fragilariopsis* spp. when the ice-free season advances (Booth et al., 2002; Vidussi et al.,  
358 2004; von Quillfeldt, 2000). Diatoms also dominated surface waters north of Cape Bathurst  
359 and near the Mackenzie estuary (cluster 1 surf) but their biomass was lower and related to  
360 different species according to microscopy (i.e. *Thalassiosira nordenskiöldii* and *Pseudo-*  
361 *nitzschia* sp.). Dominance of diatoms in cluster 1 surf showed by both, microscopy and  
362 pigment, strongly differ from the surface communities associated to the cluster 2 and  
363 characterized by green algae, dinoflagellates and haptophytes. However, environmental  
364 conditions associated to these two clusters (Table 4) were similar and cannot explain the  
365 differences in communities. We suppose that the higher dominance of diatoms in surface  
366 waters of the cluster 1 could be a remnant of past event as an upwelling. Sporadic high  
367 concentration of Chl *a* and occurrence of *Chaetoceros socialis* was previously observed in  
368 September 2005 at the SCM and at the surface following local upwelling events and advective  
369 input of nutrients from the deep basin (Comeau et al., 2011).

370 The SCM of basin stations was dominated by two distinct flagellate assemblages, which  
371 are distinguished by their Hex-fuco/But-fuco ratio. The prymnesiophytes characterized by a  
372 high Hex-fuco/But-fuco ratio ( $\approx 3$ ) dominated cluster 4 while *c*<sub>3</sub>-flagellates associated with  
373 a low Hex-fuco/But-fuco ratio ( $\approx 1$ ) dominated cluster 3. The shift in assemblages was related  
374 to the vertical position of the SCM relative to the nitracline. The prymnesiophytes, mainly  
375 associated with *Chrysochromulina* sp., dominated when the SCM matched the nitracline,  
376 whereas *c*<sub>3</sub>-flagellates dominated when the SCM was below the nitracline (Fig. 5).  
377 Incidentally, the relatively shallow prymnesiophyte-dominated SCM ( $\approx 55\text{m}$ ) was exposed to  
378 more light ( $\text{PAR} = 4.7 \pm 1.7$   $\mu\text{M m}^{-2} \text{s}^{-1}$ , Table 4) but less nitrate ( $0.5 \pm 0.2$   $\mu\text{mol L}^{-1}$ , Table 4)  
379 than the deeper *c*<sub>3</sub>-flagellate-dominated SCM ( $\approx 65\text{m}$ ) that occurred at a PAR of  
380  $2.2 \pm 1.2$   $\mu\text{M m}^{-2} \text{s}^{-1}$  and 10-fold higher nitrate concentrations ( $5.1 \pm 2.7$   $\mu\text{mol L}^{-1}$ ) and  
381 significantly higher phosphate concentrations. We stated that the *c*<sub>3</sub>-flagellate group was  
382 comprised primarily of raphidophytes. Indeed, microscopy showed that raphidophytes were

383 present only at the SCM of basin stations, where they represented 25% of phytoplankton  
384 carbon biomass (Table 2). The lack of photoprotective pigments in raphidophytes could  
385 explain why this group is restricted to deep SCM (Van den Hoek, 1995). A recent study based  
386 on molecular approaches showed an increase of prymnesiophytes type *Chrysochromulina* sp.  
387 since 2007 in the Beaufort Sea (Comeau et al., 2011). The prevalence of flagellates was  
388 attributed to the gradual freshening of the Beaufort Sea and increasing stratification. The lack  
389 of mixing may act to force the SCM deeper resulting in lower ambient PAR (McLaughlin and  
390 Carmack, 2010). Dominance of nanoflagellates has been previously noticed in SCM waters of  
391 the Canada Basin in conditions of intense freshwater accumulation (Coupel et al., 2012).

### 392 **3.4. Cell abundance and carbon biomass: implications for carbon export**

393 The chemotaxonomic interpretation of pigments remains semi-quantitative. CHEMTAX  
394 provides the percentage contribution of phytoplankton groups according to their relative  
395 contribution to TChl *a*. This information is relevant to monitor changes in the phytoplankton  
396 communities or changes in the plankton pigment composition caused by modifications in the  
397 environment as nutrients or light regimes. A change in the relative contribution of pigments is  
398 a clear indication of change in the structure or in the acclimation of phytoplankton  
399 communities. Nevertheless, to investigate the implications of phytoplankton changes on food  
400 webs and the biological pump, the pigment data must be converted into contribution to total  
401 abundance or carbon biomass. However, this conversion is not always straightforward since  
402 pigment chemotaxonomy and microscopy measure different parameters with different units  
403 (i.e. cell numbers, mg C m<sup>-3</sup> versus mg Chl *a* m<sup>-3</sup>).

404 Not surprisingly, the contribution of different phytoplankton groups to total cell  
405 abundance differed from their contribution to total phytoplankton carbon biomass. The  
406 picophytoplankton largely dominated cell abundance, except on the shelf where diatoms  
407 dominated the SCM (Fig. 6, Table 2), but contributed only 0-3% and 6-7% of the total  
408 phytoplankton carbon biomass over the shelf and basin, respectively. Phytoplankton larger  
409 than 3µm dominated carbon biomass at all stations (Fig. 7, Table 2). The minimum total  
410 phytoplankton abundance was observed at SCM of the basin (2500 ± 2500 cell mL<sup>-1</sup>) and the  
411 maximum in surface of the shelf (4400 ± 1400 cell mL<sup>-1</sup>). Nevertheless, the total  
412 phytoplankton abundance over the shelf was not significantly higher than in the Beaufort  
413 basin. Conversely, average carbon biomass at the surface was 3 times higher on the shelf (64  
414 ± 22 mg C m<sup>-3</sup>) than in the basin (25 ± 7 mg C m<sup>-3</sup>). The difference was more pronounced at  
415 the SCM, where carbon biomass was 8 times higher at shelf stations (110 ± 57 mg C m<sup>-3</sup>) than  
416 at basin stations (14 ± 5 mg C m<sup>-3</sup>). This contrast was attributed to the dominance of SCM  
417 carbon biomass (up to 90%) by diatoms on the shelf. Otherwise the carbon biomass was  
418 dominated at 50-75% by dinoflagellates, which represented less than 15% of total cell  
419 abundance (Table 2). The highest biomasses of dinoflagellates occurred in surface waters of  
420 the Mackenzie canyon area (Stations 600's, Fig. 6a, 6c) and were associated with high  
421 biomasses of other heterotrophs, mainly ciliates. Raphidophytes also made a substantial  
422 contribution (26%) to the total phytoplankton carbon biomass at the SCM of basin stations.

423 Since the estimated contributions of phytoplankton groups to carbon biomass differ from  
424 contributions to cell abundance one might ask which of the two variables should be reflected  
425 by the chemotaxonomic approach. Overall, the contribution of algal groups to TChl *a*  
426 (CHEMTAX) showed better agreement with their contribution to total cell abundance (Fig. 8)  
427 than to total carbon biomass (Fig. 9). The best agreement between CHEMTAX and relative  
428 abundance and biomass was obtained for diatoms (Fig. 8a, 9a). For nanoflagellates and  
429 picophytoplankton, CHEMTAX showed a moderate correlation with relative abundance (Fig.  
430 8b, 8c) and a weak one with relative biomass (Fig. 9b, 9c). In fact, CHEMTAX  
431 underestimates the importance of picophytoplankton and nanoflagellates in terms of cell

432 abundance but overestimates their importance in terms of carbon biomass, as shown by the  
433 position of data points with respect to the 1:1 line in Figures 8b, 8c and 9b, 9c. We observed  
434 that the contribution of picophytoplankton to TChl *a* became significant only when its  
435 contribution to total cell abundance exceeded 80% (Fig. 8b). Obviously, the underestimation  
436 of small phytoplankton abundance by chemotaxonomy is explained by the lower amount of  
437 pigment including Chl *a* in small cells compared to large cells. On the other hand, the ratio of  
438 carbon to TChl *a* (C/TChl *a*) in phytoplankton increases with cell volume (Geider et al.,  
439 1986). The fact that small cells are richer in Chl *a* than large cells for a similar carbon  
440 biomass could explain the overestimation in the contribution of small phytoplankton to total  
441 carbon biomass by the chemotaxonomy. Based on the relationships between cell volume and  
442 content in Chl *a* and carbon proposed by Montagnes et al. (1994), we calculate the ratio  
443 C/TChl *a* of a *Micromonas* sp. (1  $\mu\text{m}^3$ ) to be twice as low than in diatoms or dinoflagellates  
444 (1000  $\mu\text{m}^3$ ). Indeed, the pigments are mainly in the periphery of the cell, which means that the  
445 intracellular pigment density increases as the surface area to volume ratio increases. This is  
446 clearly demonstrated by comparing the mean C/TChl *a* ratio of the surface waters dominated  
447 by diatoms (Cluster 1 surf: C/TChl *a* = 280  $\pm$  150, Table 4), with the surface waters  
448 dominated by *Micromonas* sp. (Cluster 2, C/TChl *a* = 160  $\pm$  110). The weaker relation  
449 between CHEMTAX and carbon biomass could have been induced by these variations in the  
450 C/TChl *a* ratios of the phytoplankton and by the different transfer equations used to determine  
451 the carbon biomass from the biovolume (see section 2.3.).

452 No significant correlation was observed between CHEMTAX and microscopy for  
453 dinoflagellates, prymnesiophytes, chrysophytes, chlorophytes and cryptophytes. Such  
454 inconsistencies are mainly attributed to the low accuracy of visual counts for nano-sized  
455 flagellates. Up to 35% of the visible flagellates were categorized as unidentified and others  
456 may have been overlooked because of poor conservation. The most surprising divergence  
457 between CHEMTAX and microscopy occurred for dinoflagellates (Fig. 8d, 9d). Despite the  
458 high contribution of this group to carbon biomass (Fig. 7), it rarely contributed more than  
459 10% of the TChl *a* according to CHEMTAX. While such a discrepancy may generally arise  
460 from the large biovolume and high C/TChl *a* ratio of dinoflagellates compared to other  
461 groups, in our study it was presumably caused by the inability of CHEMTAX to detect  
462 dinoflagellates of the genera *Gymnodinium* sp. and *Gyrodinium* sp., which lack Peri (Jeffrey  
463 et al., 1997). Indeed, we found no correlation between dinoflagellate abundance and the  
464 unambiguous pigment Peri used by CHEMTAX to detect this group ( $r^2 = 0.04$ , not shown).  
465 Only the surface waters of the stations 394 and 680 dominated by an autotrophic  
466 dinoflagellate (*Heterocapsa rotundata*) known to possess a relative high Peri content showed  
467 the presence of Peri in relative high proportion. Molecular analyses indicated that the  
468 nonphotosynthetic heterotrophic species *Gyrodinium rubrum* dominated the dinoflagellate  
469 assemblages in the region (D. Onda personal communication, 2014). Heterotrophic  
470 dinoflagellates would only contain diagnostic pigments if they ingested them with their prey.  
471 It is known that heterotrophic and mixotrophic dinoflagellates feed on diverse prey items  
472 including bacteria, picoeukaryotes, nanoflagellates, diatoms, other dinoflagellates,  
473 heterotrophic protists, and metazoans due to their diverse feeding mechanisms (Jeong et al.,  
474 2010) and are likely to be significant consumers of bloom-forming diatoms (Sherr and Sherr,  
475 2007). It follows that the presence of heterotrophic dinoflagellates could potentially lead to  
476 overestimation of the phytoplanktonic groups they ingest when looking at the pigment  
477 concentrations. In contrast to the study of Brugel et al. (2009) in the Beaufort Sea during  
478 summer 2002, when autotrophic dinoflagellates contributed as much as heterotrophic  
479 dinoflagellates abundance, heterotrophic dinoflagellates were largely dominant in 2009. Strict  
480 autotrophic dinoflagellates represented only 13% of total dinoflagellate biomass.

481 The high contribution of heterotrophic dinoflagellates and ciliates in surface waters

482 suggest an important transfer of organic material to the pelagic food web and a reduced  
483 sinking export of high quality algal material, due to assimilation and remineralization as  
484 mentioned by Juul-Pedersen et al. (2010). This scenario also agrees with the observation of  
485 (Forest et al., 2014) showing a limited vertical exchange of nutrients and carbon between the  
486 surface and sub-surface and the establishment of a food web exclusively based on small  
487 protists using recycled nutrients. Conversely, the high abundance of centric diatoms at the  
488 SCM on the shelf could lead to an effective transfer of high quality algal material to the  
489 benthos as evidenced by the very large pool and fluxes of POC observed at shelf stations by  
490 (Forest et al., 2014) during the same cruise. The high abundance of Fuco previously observed  
491 in the sediment of the Mackenzie shelf during summer supports the hypothesis of an efficient  
492 export of diatoms to the seafloor (Morata et al., 2008).

#### 493 **4. Conclusion**

494 We evaluated the utility of CHEMTAX to characterize phytoplankton dynamics in the  
495 Beaufort Sea in late summer 2009. Based on the taxonomic information from optical  
496 microscopy, a **ratio matrix** was created specifically for the Beaufort Sea and run using the  
497 CHEMTAX software.

498 The interpretation of the pigment data by CHEMTAX highlights linkages between the  
499 phytoplankton distribution and environmental parameters commonly **observed in the Arctic**  
500 Ocean. The productive and nutrient rich sub-surface waters of the shelf were dominated (95%  
501 of abundance) by the centric diatom identified by microscopy as *Chaetoceros socialis*. In  
502 contrast, oligotrophic, nutrient-depleted surface waters over the shelf and basin presented the  
503 highest contribution of green algae (48% of the TChl *a*), dominated by the pico-prasinophytes  
504 *Micromonas* sp.

505 The use of pigments and CHEMTAX also revealed more subtle information difficult to  
506 observe with other taxonomic methods. Indeed, two populations of flagellates were  
507 highlighted in sub-surface waters of the basin: prymnesiophytes, rich in Hex-Fuco pigment,  
508 and a group of various flagellates rich in Chl *c*<sub>3</sub> and Fuco (i.e. *c*<sub>3</sub>-flagellates). The  
509 prymnesiophytes dominated where the sub-surface chlorophyll maximum was located above  
510 60 m and were associated with higher light availability and lower nutrient concentrations. In  
511 contrast, the *c*<sub>3</sub>-flagellates dominated when the sub-surface chlorophyll maximum was deeper  
512 than 60 m and the organisms were exposed to higher nitrate concentrations and lower light.  
513 Flagellate populations that are able to grow **at deep sub-surface chlorophyll *a* maxima** should  
514 be closely monitored in a context **of a deepening nutricline** observed **over the past decade** in  
515 the Canadian Arctic due to increased surface freshening and stratification.

516 The present study underlines the high sensitivity of CHEMTAX to the initial **ratio matrix**  
517 chosen and the misinterpretation **introduced** by a blind use of a **ratio matrix** calibrated in  
518 regions other than the targeted one. Therefore, we recommend that future pigment studies in  
519 the Beaufort Sea use the CHEMTAX parameterization developed in the present work.

520 However, some issues and inconsistencies should be considered when using CHEMTAX in  
521 the Beaufort Sea and, probably, in the entire Arctic Ocean. Despite high biomasses, the  
522 heterotrophic dinoflagellates of the Gymnodinium/Gyrodinium complex were undetected by  
523 pigment analyses since they lack peridinin. High heterotrophy can lead to misinterpretation  
524 because CHEMTAX potentially takes into account other pigments present in the algae  
525 ingested by dinoflagellates. Additionally, CHEMTAX underestimates the importance of small  
526 phytoplankton in terms of cell abundance but overestimates their importance in terms of  
527 carbon biomass. The variability in pigment content per cell and in the C/TChl *a* ratio makes it  
528 difficult to relate pigment signatures to carbon biomass or cell abundance. The contribution of  
529 small phytoplankton to TChl *a* was 2 to 3 times higher than their contribution to carbon  
530 biomass due to generally low C/TChl *a* ratios of these organisms. The opposite was observed

531 for large phytoplankton like dinoflagellates for which contribution to total biomass was higher  
532 than their contribution to TChl *a*. Overall, we found the contribution of algal groups to TChl *a*  
533 (CHEMTAX) showed better agreement with their contribution to total cell abundance than  
534 their contribution to the total phytoplankton carbon biomass.

535 In contrast, for localized use of CHEMTAX, as presented in our study, the large  
536 pigment dataset **in the Arctic Ocean** could be used to determine **average** pigment ratios for the  
537 dominant Arctic phytoplankton groups and create a single pan-Arctic **ratio matrix** for  
538 CHEMTAX. With this goal in mind, we advise creating a simple **ratio matrix** in CHEMTAX  
539 to retrieve the three functional groups diatoms, nanoflagellates and picophytoplankton  
540 successfully validated by optical microscopy. Indeed, a weak or no correlation was found  
541 between CHEMTAX and microscopy for the other groups: chrysophytes, prymnesiophytes,  
542 chlorophytes and cryptophytes. Nonetheless, we attribute these dissimilarities to the high  
543 proportion of flagellates that are unidentified or overlooked by microscopy rather than a  
544 misinterpretation by CHEMTAX.

545 Alternatively, when taxonomic information is lacking in the targeted study area, we  
546 recommend using the raw pigment data and selecting key pigment ratios **rather than use a**  
547 **CHEMTAX parameterization tuned for a different region.** The high reproducibility of the  
548 HPLC method for pigment measurements and a local CHEMTAX calibration would provide a  
549 suitable approach to detect inter-annual changes in the phytoplankton communities.  
550 Nevertheless, pigment-derived information gains in accuracy when coupled with other  
551 measurements type. The optical microscopy and flow cytometry remain crucial to convert the  
552 phytoplankton into carbon budget or to detect heterotrophic plankton groups as the  
553 **dinoflagellates.**

554  
555 *Acknowledgements.* This study was conducted as part of the Malina Scientific Program led by  
556 Marcel Babin and funded by ANR (Agence nationale de la recherche), INSU-CNRS (Institut  
557 national des sciences de l'Univers – Centre national de la recherche scientifique), CNES  
558 (Centre national d'études spatiales) and ESA (European Space Agency). The present study  
559 started at the LOCEAN laboratory (UPMC – University Pierre et Marie Curie) supported by  
560 the Arctic Tipping Point project (ATP, <http://www.eu-atp.org>) funded by FP7 of the European  
561 Union (contract #226248) and was continued at Laval University (Quebec, Canada) funded  
562 by the Canada Excellence Research Chair in “Remote sensing of Canada’s new Arctic  
563 frontier” and Québec-Océan. We are grateful to the crew and captain of the Canadian research  
564 icebreaker CCGS *Amundsen*. Thanks to S. Lessard for the phytoplankton identification and  
565 enumeration by light microscopy and to H. Claustre and J.Ras for the pigment analyses.

566  
567  
568 **Alou-Font, E., Mundy, C. J., Roy, S., Gosselin, M., and Agustí, S.: Snow cover affects ice algal pigment**  
569 **composition in the coastal Arctic Ocean during spring, *Marine Ecology Progress Series*, 474, 89-104, 2013.**

570 **Alvain, S., Moulin, C., Dandonneau, Y., and Breon, F. M.: Remote sensing of phytoplankton groups in**  
571 **case 1 waters from global SeaWiFS imagery, *Deep-Sea Research Part I-Oceanographic Research Papers*,**  
572 **52, 1989-2004, 2005.**

573 **Ansotegui, A., Trigueros, J., and Orive, E.: The use of pigment signatures to assess phytoplankton**  
574 **assemblage structure in estuarine waters, *Estuarine, Coastal and Shelf Science*, 52, 689-703, 2001.**

575 **Balzano, S., Marie, D., Gourvil, P., and Vaultot, D.: Composition of the summer photosynthetic pico and**  
576 **nanoplankton communities in the Beaufort Sea assessed by T-RFLP and sequences of the 18S rRNA gene**  
577 **from flow cytometry sorted samples, *ISME J*, 6, 1480-1498, 2012.**

- 578 Bérard-Therriault, L., Poulin, M., and Bossé, L.: Guide d'identification du phytoplancton marin de  
579 l'estuaire et du golfe du Saint-Laurent: incluant également certains protozoaires, Publ. spéc. can. sci.  
580 halieut. aquat., 1999.
- 581 Bidigare, R. R., Frank, T. J., Zastrow, C., and Brooks, J. M.: The distribution of algal chlorophylls and  
582 their degradation products in the Southern Ocean, Deep Sea Research Part A. Oceanographic Research  
583 Papers, 33, 923-937, 1986.
- 584 Booth, B. C., Larouche, P., Bélanger, S., Klein, B., Amiel, D., and Mei, Z. P.: Dynamics of *Chaetoceros*  
585 *socialis* blooms in the North Water, Deep Sea Research Part II: Topical Studies in Oceanography, 49,  
586 5003-5025, 2002.
- 587 Brugel, S., Nozais, C., Poulin, M., Tremblay, J. E., Miller, L. A., Simpson, K. G., Gratton, Y., and Demers,  
588 S.: Phytoplankton biomass and production in the southeastern Beaufort Sea in autumn 2002 and 2003,  
589 Marine Ecology Progress Series, 377, 63-77, 2009.
- 590 Carmack, E. and Wassmann, P.: Food webs and physical-biological coupling on pan-Arctic shelves:  
591 Unifying concepts and comprehensive perspectives, Progress in Oceanography, 71, 446-477, 2006.
- 592 Carmack, E. C., Macdonald, R. W., and Jasper, S.: Phytoplankton productivity on the Canadian Shelf of  
593 the Beaufort Sea, Marine Ecology Progress Series, 277, 37-50, 2004.
- 594 Comeau, A. M., Li, W. K., Tremblay, J. E., Carmack, E. C., and Lovejoy, C.: Arctic Ocean microbial  
595 community structure before and after the 2007 record sea ice minimum, PLoS ONE, 6, e27492,  
596 doi:10.1371/journal.pone.0027492, 2011.
- 597 Comiso, J. C., Parkinson, C. L., Gersten, R., and Stock, L.: Accelerated decline in the Arctic sea ice cover,  
598 Geophysical Research Letters, 35, L01703, doi:10.1029/2007GL031972, 2008.
- 599 Coupel, P., Jin, H. Y., Joo, M., Horner, R., Bouvet, H. A., Sicre, M. A., Gascard, J. C., Chen, J. F.,  
600 Garçon, V., and Ruiz-Pino, D.: Phytoplankton distribution in unusually low sea ice cover over the Pacific  
601 Arctic, Biogeosciences, 9, 4835-4850, 2012.
- 602 Del Campo, J. A., Moreno, J., Rodriguez, H., Vargas, M. A., Rivas, J., and Guerrero, M. G.: Carotenoid  
603 content of chlorophycean microalgae: factors determining lutein accumulation in *Muriellopsis* sp.  
604 (*Chlorophyta*), J Biotechnol, 76, 51-59, 2000.
- 605 Demers, S., Roy, S., Gagnon, R., and Vignault, C.: Rapid Light-Induced-Changes in Cell Fluorescence  
606 and in Xanthophyll-Cycle Pigments of *Alexandrium-Excavatum* (*Dinophyceae*) and *Thalassiosira-*  
607 *Pseudonana* (*Bacillariophyceae*) - a Photo-Protection Mechanism, Marine Ecology Progress Series, 76,  
608 185-193, 1991.
- 609 Falkowski, P.: The Global Carbon Cycle: A Test of Our Knowledge of Earth as a System, Science, 290,  
610 291-296, 2000.
- 611 Forest, A., Coupel, P., Else, B., Nahavandian, S., Lansard, B., Raimbault, P., Papakyriakou, T., Gratton,  
612 Y., Fortier, L., and Tremblay, J.-É.: Synoptic evaluation of carbon cycling in the Beaufort Sea during  
613 summer: contrasting river inputs, ecosystem metabolism and air-sea CO<sub>2</sub> fluxes, Biogeosciences, 11,  
614 2827-2856, 2014.
- 615 Frank, H. A., Cua, A., Chynwat, V., Young, A., Gosztola, D., and Wasielowski, M. R.: Photophysics of the  
616 carotenoids associated with the xanthophyll cycle in photosynthesis, Photosynthesis Research, 41, 389-395,  
617 1994.
- 618 Fujiki, T. and Taguchi, S.: Variability in chlorophyll a specific absorption coefficient in marine  
619 phytoplankton as a function of cell size and irradiance, Journal of Plankton Research, 24, 859-874, 2002.
- 620 Geider, R., Platt, T., and Raven, J. A.: Size dependence of growth and photosynthesis in diatoms: a  
621 synthesis, Mar. Ecol. Prog. Ser, 30, 93-104, 1986.

- 622 Grebmeier, J. M., Moore, S. E., Overland, J. E., Frey, K. E., and Gradinger, R.: Biological Response to  
623 Recent Pacific Arctic Sea Ice Retreats, *Eos Trans. AGU*, 91, 161–168, 2010.
- 624 Higgins, H., Wright, S., and Schluter, L.: Quantitative interpretation of chemotaxonomic pigment data,  
625 2011. 2011.
- 626 Hill, V., Cota, G., and Stockwell, D.: Spring and summer phytoplankton communities in the Chukchi and  
627 Eastern Beaufort Seas, *Deep Sea Research Part II: Topical Studies in Oceanography*, 52, 3369-3385, 2005.
- 628 Hirata, T., Hardman-Mountford, N. J., Brewin, R. J. W., Aiken, J., Barlow, R., Suzuki, K., Isada, T.,  
629 Howell, E., Hashioka, T., Noguchi-Aita, M., and Yamanaka, Y.: Synoptic relationships between surface  
630 Chlorophyll-*a* and diagnostic pigments specific to phytoplankton functional types, *Biogeosciences*, 8, 311-  
631 327, 2011.
- 632 Hooker, S. B., Van Heukelem, L., Thomas, C. S., Claustre, H., Ras, J., Barlow, R., Sessions, H., Schlüter,  
633 L., Perl, J., and Trees, C.: Second SeaWiFS HPLC Analysis Round-robin Experiment (SeaHARRE-2),  
634 National Aeronautics and Space Administration, Goddard Space Flight Center, 2005.
- 635 Hunt Jr, G. L., Stabeno, P., Walters, G., Sinclair, E., Brodeur, R. D., Napp, J. M., and Bond, N. A.:  
636 Climate change and control of the southeastern Bering Sea pelagic ecosystem, *Deep Sea Research Part II:*  
637 *Topical Studies in Oceanography*, 49, 5821-5853, 2002.
- 638 Irigoien, X., Meyer, B., Harris, R., and Harbour, D.: Using HPLC pigment analysis to investigate  
639 phytoplankton taxonomy: the importance of knowing your species, *Helgol Mar Res*, 58, 77-82, 2004.
- 640 Jeffrey, S. W., Mantoura, R. F. C., and Wright, S. W.: Phytoplankton pigments in oceanography,  
641 *Monographs on oceanographic methods*. UNESCO, Paris, 1997..
- 642 Jeong, H., Yoo, Y., Kim, J., Seong, K., Kang, N., and Kim, T.: Growth, feeding and ecological roles of the  
643 mixotrophic and heterotrophic dinoflagellates in marine planktonic food webs, *Ocean Sci. J.*, 45, 65-91,  
644 2010.
- 645 Juul-Pedersen, T., Michel, C., and Gosselin, M.: Sinking export of particulate organic material from the  
646 euphotic zone in the eastern Beaufort Sea, *Marine Ecology Progress Series*, 410, 55-70, 2010.
- 647 Kozlowski, W. A., Deutschman, D., Garibotti, I., Trees, C., and Vernet, M.: An evaluation of the  
648 application of CHEMTAX to Antarctic coastal pigment data, *Deep Sea Research Part I: Oceanographic*  
649 *Research Papers*, 58, 350-364, 2011.
- 650 Lewitus, A. J., White, D. L., Tymowski, R. G., Geesey, M. E., Hymel, S. N., and Noble, P. A.: Adapting the  
651 CHEMTAX method for assessing phytoplankton taxonomic composition in southeastern US estuaries,  
652 *Estuaries*, 28, 160-172, 2005.
- 653 Li, W. K., McLaughlin, F. A., Lovejoy, C., and Carmack, E. C.: Smallest algae thrive as the Arctic Ocean  
654 freshens, *Science*, 326, 539, 2009.
- 655 Lovejoy, C., Vincent, W. F., Bonilla, S., Roy, S., Martineau, M.-J., Terrado, R., Potvin, M., Massana, R.,  
656 and Pedrós-Alió, C.: Distribution, Phylogeny, and Growth of Cold-Adapted Picoprasinophytes in Arctic  
657 Seas, *Journal of Phycology*, 43, 78-89, 2007.
- 658 Lund, J. W. G., Kipling, C., and Cren, E. D.: The inverted microscope method of estimating algal  
659 numbers and the statistical basis of estimations by counting, *Hydrobiologia*, 11, 143-170, 1958.
- 660 Mackey, M. D., Mackey, D. J., Higgins, H. W., and Wright, S. W.: CHEMTAX - a program for estimating  
661 class abundances from chemical markers: application to HPLC measurements of phytoplankton, *Marine*  
662 *Ecology Progress Series*, 144, 265-283, 1996.
- 663 MacQueen, J.: Some methods for classification and analysis of multivariate observations, 1967, 14.

- 664 Marie, D., Partensky, F., Jacquet, S., and Vaultot, D.: Enumeration and cell cycle analysis of natural  
665 populations of marine picoplankton by flow cytometry using the nucleic acid stain SYBR Green I, *Applied*  
666 *and environmental microbiology*, 63, 186-193, 1997.
- 667 McLaughlin, F. A. and Carmack, E. C.: Deepening of the nutricline and chlorophyll maximum in the  
668 Canada Basin interior, 2003–2009, *Geophysical Research Letters*, 37, L24602, doi:10.1029/2010GL045459,  
669 2010.
- 670 Menden-Deuer, S. and Lessard, E. J.: Carbon to volume relationships for dinoflagellates, diatoms, and  
671 other protist plankton, *American Society of Limnology and Oceanography*, Waco, TX, ETATS-UNIS,  
672 2000.
- 673 Montagnes, D. J., Berges, J. A., Harrison, P. J., and Taylor, F.: Estimating carbon, nitrogen, protein, and  
674 chlorophyll a from volume in marine phytoplankton, *Limnology and Oceanography*, 39, 1044-1060, 1994.
- 675 Morata, N., Renaud, P. E., Brugel, S., Hobson, K. A., and Johnson, B. J.: Spatial and seasonal variations  
676 in the pelagic–benthic coupling of the southeastern Beaufort Sea revealed by sedimentary biomarkers,  
677 *Marine Ecology Progress Series*, 371, 47-63, 2008.
- 678 Not, F., Ramon, M., Latasa, M., Marie, D., Colson, C., Eikrem, W., Pedrós-Alió, C., Vaultot, D., and  
679 Simon, N.: Late Summer Community Composition and Abundance of Photosynthetic Picoeukaryotes in  
680 Norwegian and Barents Seas, *Limnology and Oceanography*, 50, 1677-1686, 2005.
- 681 Olenina, I., Hajdu, S., Edler, L., Andersson, A., Wasmund, N., Busch, S., Göbel, J., Gromisz, S., Huseby,  
682 S., Huttunen, M., Jaanus, A., Kokkonen, P., Ledaine, I., and Niemkiewicz, E.: Biovolumes and size-classes  
683 of phytoplankton in the Baltic Sea. Baltic Marine Environment Protection Commission - HELCOM,  
684 Helsinki, 2006.
- 685 Pickart, R. S., Schulze, L. M., Moore, G. W. K., Charette, M. A., Arrigo, K. R., van Dijken, G., and  
686 Danielson, S. L.: Long-term trends of upwelling and impacts on primary productivity in the Alaskan  
687 Beaufort Sea, *Deep Sea Research Part I: Oceanographic Research Papers*, 79, 106-121, 2013.
- 688 Poulin, M., Daugbjerg, N., Gradinger, R., Ilyash, L., Ratkova, T., and Quillfeldt, C.: The pan-Arctic  
689 biodiversity of marine pelagic and sea-ice unicellular eukaryotes: a first-attempt assessment, *Marine*  
690 *Biodiversity*, 41, 13-28, 2010.
- 691 Riegman, R. and Kraay, G. W.: Phytoplankton community structure derived from HPLC analysis of  
692 pigments in the Faroe-Shetland Channel during summer 1999: the distribution of taxonomic groups in  
693 relation to physical/chemical conditions in the photic zone, *Journal of Plankton Research*, 23, 191-205,  
694 2001.
- 695 Rodriguez, F., Varela, M., and Zapata, M.: Phytoplankton assemblages in the Gerlache and Bransfield  
696 Straits (Antarctic Peninsula) determined by light microscopy and CHEMTAX analysis of HPLC pigment  
697 data, *Deep Sea Research Part II: Topical Studies in Oceanography*, 49, 723-747, 2002.
- 698 Rothrock, D. A., Yu, Y., and Maykut, G. A.: Thinning of the Arctic sea-ice cover, *Geophysical Research*  
699 *Letters*, 26, 3469-3472, 1999.
- 700 Roy, S., Chanut, J.-P., Gosselin, M., and Sime-Ngando, T.: Characterization of phytoplankton  
701 communities in the lower St. Lawrence Estuary using HPLC-detected pigments and cell microscopy, *Mar*  
702 *Ecol Prog Ser*, 142, 55-73, 1996.
- 703 Sathyendranath, S., Watts, L., Devred, E., Platt, T., Caverhill, C., and Maass, H.: Discrimination of  
704 diatoms from other phytoplankton using ocean-colour data, *Marine Ecology Progress Series*, 272, 59-68,  
705 2004.
- 706 Schlüter, L., Möhlenberg, F., Havskum, H., and Larsen, S.: The use of phytoplankton pigments for  
707 identifying and quantifying phytoplankton groups in coastal areas: testing the influence of light and  
708 nutrients on pigment/chlorophyll a ratios, *Marine Ecology Progress Series*, 192, 49-63, 2000.

- 709 Sherr, E. B. and Sherr, B. F.: Heterotrophic dinoflagellates: a significant component of microzooplankton  
710 biomass and major grazers of diatoms in the sea, *Mar. Ecol.-Prog. Ser.*, 352, 187–197,  
711 doi:10.3354/meps07161, 2007.
- 712
- 713 Sigman, D. M. and Boyle, E. A.: Glacial/interglacial variations in atmospheric carbon dioxide, *Nature*,  
714 407, 859-869, 2000.
- 715
- 716 Stroeve, J. C., Serreze, M. C., Holland, M. M., Kay, J. E., Malanik, J., and Barrett, A. P.: The Arctic's  
717 rapidly shrinking sea ice cover: a research synthesis, *Climatic Change*, 110, 1005-1027, 2011.
- 718
- 719 Suzuki, K., Minami, C., Liu, H., and Saino, T.: Temporal and spatial patterns of chemotaxonomic algal  
720 pigments in the subarctic Pacific and the Bering Sea during the early summer of 1999, *Deep Sea Research*  
721 *Part II: Topical Studies in Oceanography*, 49, 5685-5704, 2002.
- 722
- 723 Taylor, R. L., Semeniuk, D. M., Payne, C. D., Zhou, J., Tremblay, J.-É., Cullen, J. T., and Maldonado, M.  
724 T.: Colimitation by light, nitrate, and iron in the Beaufort Sea in late summer, *Journal of Geophysical*  
725 *Research: Oceans*, 118, 3260-3277, 2013.
- 726
- 727 Tremblay, J. E., Belanger, S., Barber, D. G., Asplin, M., Martin, J., Darnis, G., Fortier, L., Gratton, Y.,  
728 Link, H., Archambault, P., Sallon, A., Michel, C., Williams, W. J., Philippe, B., and Gosselin, M.: Climate  
729 forcing multiplies biological productivity in the coastal Arctic Ocean, *Geophys. Res. Lett.*, 38, L18604,  
730 doi:10.1029/2011GL048825, 2011.
- 731
- 732 Uitz, J., Claustre, H., Morel, A., and Hooker, S. B.: Vertical distribution of phytoplankton communities in  
733 open ocean: An assessment based on surface chlorophyll, *J. Geophys. Res.*, 111,  
734 doi:10.1029/2005JC003207, 2006.
- 735
- 736 Van den Hoek, C.: *Algae: an introduction to phycology*, Cambridge University Press, 1995.
- 737
- 738 Van Heukelem, L. and Thomas, C. S.: Computer-assisted high-performance liquid chromatography  
739 method development with applications to the isolation and analysis of phytoplankton pigments, *Journal of*  
740 *Chromatography A*, 910, 31-49, 2001.
- 741
- 742 Vidussi, F., Roy, S., Lovejoy, C., Gammelgaard, M., Thomsen, H., Booth, B., Tremblay, J. E., and  
743 Mostajir, B.: Spatial and temporal variability of the phytoplankton community structure in the North  
744 Water Polynya, investigated using pigment biomarkers, *Canadian Journal of Fisheries and Aquatic*  
745 *Sciences*, 61, 2038-2052, 2004.
- 746
- 747 von Quillfeldt, C. H.: Common Diatom Species in Arctic Spring Blooms: Their Distribution and  
748 Abundance. In: *Botanica Marina*, 6, 2000.
- 749
- 750 Wassmann, P., Duarte, C. M., Agusti, S., and Sejr, M. K.: Footprints of climate change in the Arctic  
751 marine ecosystem, *Global Change Biology*, 17, 1235-1249, 2011.
- 752
- 753 Wassmann, P. and Reigstad, M.: Future Arctic Ocean Seasonal Ice Zones and Implications for Pelagic-  
754 Benthic Coupling, *Oceanography*, 24, 220-231, 2011.
- 755
- 756 Wright, S. W. and Jeffrey, S. W.: Pigment Markers for Phytoplankton Production. In: *Marine Organic*  
757 *Matter: Biomarkers, Isotopes and DNA*, Volkman, J. (Ed.), The Handbook of Environmental Chemistry,  
758 Springer Berlin Heidelberg, 2006.
- 759
- 760 Wright, S. W., Thomas, D. P., Marchant, H. J., Higgins, H. W., Mackey, M. D., and Mackey, D. J.:  
761 Analysis of phytoplankton of the Australian sector of the Southern Ocean: Comparisons of microscopy  
762 and size frequency data with interpretations of pigment HPLC data using the 'CHEMTAX' matrix  
763 factorisation program, *Mar. Ecol.-Prog. Ser.*, 144, 285-298, 1996.
- 764
- 765
- 766
- 767
- 768
- 769
- 770
- 771
- 772
- 773
- 774
- 775
- 776
- 777
- 778
- 779
- 780
- 781
- 782
- 783
- 784
- 785
- 786
- 787
- 788
- 789
- 790
- 791
- 792
- 793
- 794
- 795
- 796
- 797
- 798
- 799
- 800

755 **Table 1.** Distribution of major taxonomically significant pigments in algal classes using  
 756 SCOR abbreviations (Jeffrey et al., 1997).  
 757

<b>Pigment</b>	<b>Abbreviation</b>	<b>Specificity</b>
<b>Chlorophylls</b>		
Chlorophyll <i>a</i>	<b>Chl <i>a</i></b>	All photosynthetic algae
Bacteriochlorophyll <i>a</i>	<b>BChl <i>a</i></b>	Photosynthetic bacteria
Chlorophyll <i>b</i>	<b>Chl <i>b</i></b>	Dominant in green algae
Chlorophyll <i>c</i> <sub>1</sub> + <i>c</i> <sub>2</sub>	<b>Chl <i>c</i><sub>1</sub>+<i>c</i><sub>2</sub></b>	Minor in red algae
Chlorophyll <i>c</i> <sub>3</sub>	<b>Chl <i>c</i><sub>3</sub></b>	Dominant in haptophyte, many diatoms and some dinoflagellates
Chlorophyllide <i>a</i>	<b>Chlide <i>a</i></b>	Degradation products of chlorophyll <i>a</i>
Pheophorbide <i>a</i>	<b>Pheide <i>a</i></b>	Degradation products of chlorophyll <i>a</i>
Pheophytin <i>a</i>	<b>Phe <i>a</i></b>	Degradation products of chlorophyll <i>a</i>
<b>Carotene(s)</b>	<b>Car</b>	Dominant in chlorophytes, prasinophytes, minor in all other algal groups
<b>Xanthophylls</b>		
Alloxanthin	<b>Allo</b>	Major in Cryptophytes
19'-butanoyloxyfucoxanthin	<b>But-fuco</b>	Dominant in pelagophytes, dictyochophytes. Present in some haptophytes
Diadinoxanthin	<b>Diadino</b>	Diatoms, haptophytes, pelagophytes, dictyochophytes and some dinoflagellates
Diatoxanthin	<b>Diato</b>	Diatoms, haptophytes, pelagophytes, dictyochophytes and some dinoflagellates
Fucoxanthin	<b>Fuco</b>	Dominant in most red algae
19'-hexanoyloxyfucoxanthin	<b>Hex-fuco</b>	Major in Haptophytes and dinoflagellates Type 2* (lacking Peridinin)
Lutein	<b>Lut</b>	Chlorophytes, prasinophytes
Neoxanthin	<b>Neo</b>	Chlorophytes, prasinophytes
Peridinin	<b>Peri</b>	Dinoflagellates Type 1*
Prasincoxanthin	<b>Pras</b>	Prasinophytes Type 3A and 3B
Violaxanthin	<b>Viola</b>	Dominant in chlorophytes, prasinophytes, chrysophytes, some dinoflagellates
Zeaxanthin	<b>Zea</b>	Dominant in cyanobacteria, pelagophytes, chrysophytes, some dinoflagellates

758 \*Higgins et al., 2011

759

760 **Table 2.** Abundance and carbon biomass (mean  $\pm$  standard deviation) of the major protist  
761 groups in surface and subsurface chlorophyll *a* maximum (SCM) depth of the Mackenzie  
762 shelf and deep waters of the Beaufort Sea. The mean percent contribution of each protist  
763 group to total cell abundance and total carbon biomass is indicated in parenthesis. Large  
764 (> 3  $\mu\text{m}$ ) and small (< 3  $\mu\text{m}$ ) cells were counted by light microscopy and flow cytometry,  
765 respectively. The average cell abundance and carbon biomass are in bold characters. Total  
766 chlorophyll *a* concentration (mean  $\pm$  standard deviation) is indicated at the bottom of the  
767 Table. The heterotrophic group is composed of flagellated protozoans.  
768

	Mackenzie Shelf		Beaufort Sea	
	Surface (3 m)	SCM (35 $\pm$ 8 m)	Surface (3 m)	SCM (61 $\pm$ 7 m)
<i>Number of stations</i>	<i>N = 8</i>	<i>N = 6</i>	<i>N = 13</i>	<i>N = 13</i>
<b>TOTAL ABUNDANCE (cells mL<sup>-1</sup>)</b>	<b>4500 <math>\pm</math> 1400</b>	<b>4000 <math>\pm</math> 1500</b>	<b>4400 <math>\pm</math> 1400</b>	<b>2500 <math>\pm</math> 2500</b>
<b>Algae &gt;3 <math>\mu\text{m}</math></b>	<b>660 <math>\pm</math> 830 (15.0)</b>	<b>3000 <math>\pm</math> 900 (74.1)</b>	<b>140 <math>\pm</math> 140 (3.2)</b>	<b>93 <math>\pm</math> 110 (3.8)</b>
Diatoms	410 $\pm$ 610 (61.2)	2900 $\pm$ 790 (97.5)	7.1 $\pm$ 5.7 (5)	8 $\pm$ 11 (8.5)
Dinoflagellates	44 $\pm$ 30 (6.6)	8.4 $\pm$ 4.8 (0.3)	19 $\pm$ 15 (13.1)	11 $\pm$ 5 (11.9)
Chlorophytes	0.6 $\pm$ 0.9 (0.1)	0.1 $\pm$ 0.3 (0)	0.2 $\pm$ 0.4 (0.1)	0.0 $\pm$ 0.1 (0)
Chrysophytes	36 $\pm$ 39 (5.4)	4.9 $\pm$ 10.0 (0.2)	5.4 $\pm$ 6.3 (3.8)	0.1 $\pm$ 0.2 (0.1)
Dictyochophytes	18 $\pm$ 28 (2.6)	0.7 $\pm$ 1.7 (0)	9.5 $\pm$ 9.4 (6.7)	0.5 $\pm$ 0.9 (0.5)
Cryptophytes	19 $\pm$ 23 (2.8)	5.6 $\pm$ 7.0 (0.2)	4.6 $\pm$ 5.2 (3.3)	7 $\pm$ 20 (7.4)
Euglenophytes	0.2 $\pm$ 0.4 (0)	0.1 $\pm$ 0.1 (0)	0.2 $\pm$ 0.5 (0.1)	0.1 $\pm$ 0.1 (0.1)
Prasinophytes	21 $\pm$ 27 (3.2)	0.4 $\pm$ 0.4 (0)	30 $\pm$ 38 (21.2)	0.7 $\pm$ 1.5 (0.8)
Prymnesiophytes	15 $\pm$ 25 (2.3)	4.0 $\pm$ 5.5 (0.1)	19 $\pm$ 22 (13.7)	22 $\pm$ 25 (24.3)
Unidentified flagellates	100 $\pm$ 40 (15.7)	48 $\pm$ 36 (1.6)	46 $\pm$ 33 (32.8)	37 $\pm$ 41 (39.9)
Raphidophytes	0 $\pm$ 0 (0)	0.5 $\pm$ 0.5 (0)	0.0 $\pm$ 0.1 (0)	6.0 $\pm$ 6.2 (6.5)
<b>Algae &lt;3 <math>\mu\text{m}</math></b>	<b>3600 <math>\pm</math> 1500 (81.2)</b>	<b>930 <math>\pm</math> 850 (23.5)</b>	<b>4000 <math>\pm</math> 1200 (91.7)</b>	<b>2200 <math>\pm</math> 1300 (91.1)</b>
<b>Heterotrophs &gt;3 <math>\mu\text{m}</math></b>	<b>40 <math>\pm</math> 60 (0.9)</b>	<b>12 <math>\pm</math> 14 (0.3)</b>	<b>27 <math>\pm</math> 39 (0.6)</b>	<b>2.7 <math>\pm</math> 2.4 (0.1)</b>
<b>Unidentified cells &gt;3 <math>\mu\text{m}</math></b>	<b>120 <math>\pm</math> 120 (2.8)</b>	<b>86 <math>\pm</math> 44 (2.2)</b>	<b>190 <math>\pm</math> 270 (4.4)</b>	<b>120 <math>\pm</math> 160 (5.0)</b>
<b>TOTAL BIOMASS (mg C m<sup>-3</sup>)</b>	<b>64 <math>\pm</math> 22</b>	<b>110 <math>\pm</math> 57</b>	<b>25 <math>\pm</math> 7</b>	<b>14 <math>\pm</math> 5</b>
<b>Algae &gt;3 <math>\mu\text{m}</math></b>	<b>43 <math>\pm</math> 40 (54.7)</b>	<b>100 <math>\pm</math> 46 (86.8)</b>	<b>12 <math>\pm</math> 10 (39.5)</b>	<b>9.2 <math>\pm</math> 7.6 (48.5)</b>
Diatoms	15 $\pm$ 17 (35.9)	91 $\pm$ 40 (89.2)	0.51 $\pm$ 0.37 (5)	0.31 $\pm$ 0.53 (3.8)
Dinoflagellates	23 $\pm$ 20 (56.7)	9.7 $\pm$ 4.8 (9.5)	7.93 $\pm$ 6.49 (76.9)	4.63 $\pm$ 3.22 (57.3)
Chlorophytes	0.10 $\pm$ 0.21 (0.3)	0.00 $\pm$ 0.00 (0)	0.04 $\pm$ 0.11 (0.4)	0.00 $\pm$ 0.01 (0)
Chrysophytes	0.48 $\pm$ 0.33 (1.2)	0.09 $\pm$ 0.18 (0.1)	0.32 $\pm$ 0.62 (3.2)	0.00 $\pm$ 0.01 (0)
Dictyochophytes	0.15 $\pm$ 0.24 (0.4)	0.01 $\pm$ 0.03 (0)	0.09 $\pm$ 0.09 (0.9)	0.00 $\pm$ 0.01 (0)
Cryptophytes	0.28 $\pm$ 0.33 (0.7)	0.29 $\pm$ 0.45 (0.3)	0.04 $\pm$ 0.05 (0.4)	0.03 $\pm$ 0.06 (0.4)
Euglenophytes	0.04 $\pm$ 0.06 (0.1)	0.02 $\pm$ 0.04 (0)	0.07 $\pm$ 0.16 (0.7)	0.14 $\pm$ 0.36 (1.7)
Prasinophytes	0.31 $\pm$ 0.35 (0.8)	0.01 $\pm$ 0.01 (0)	0.49 $\pm$ 0.60 (4.8)	0.02 $\pm$ 0.04 (0.2)
Prymnesiophytes	0.13 $\pm$ 0.19 (0.3)	0.04 $\pm$ 0.05 (0)	0.19 $\pm$ 0.21 (1.9)	0.36 $\pm$ 0.53 (4.5)
Unidentified flagellates	1.52 $\pm$ 0.60 (3.7)	0.57 $\pm$ 0.30 (0.6)	0.60 $\pm$ 0.40 (5.8)	0.48 $\pm$ 0.45 (6)
Raphidophytes	0 $\pm$ 0 (0)	0.29 $\pm$ 0.29 (0.3)	0.01 $\pm$ 0.02 (0.1)	2.10 $\pm$ 1.68 (26)
<b>Algae &lt;3 <math>\mu\text{m}</math></b>	<b>1.9 <math>\pm</math> 0.8 (2.4)</b>	<b>0.49 <math>\pm</math> 0.45 (0.4)</b>	<b>2.1 <math>\pm</math> 0.7 (6.7)</b>	<b>1.2 <math>\pm</math> 0.7 (6.2)</b>
<b>Heterotrophs &gt;3 <math>\mu\text{m}</math></b>	<b>15 <math>\pm</math> 24 (19.3)</b>	<b>5.4 <math>\pm</math> 5.6 (4.6)</b>	<b>6.3 <math>\pm</math> 10.6 (20.2)</b>	<b>1.0 <math>\pm</math> 1.2 (5.3)</b>
<b>Unidentified cells &gt;3 <math>\mu\text{m}</math></b>	<b>3.8 <math>\pm</math> 4.0 (4.9)</b>	<b>2.3 <math>\pm</math> 2.1 (2.0)</b>	<b>4.0 <math>\pm</math> 4.4 (12.9)</b>	<b>2.9 <math>\pm</math> 3.6 (15.4)</b>
<b>TOTAL Chlorophyll <i>a</i> (mg m<sup>-3</sup>)</b>	<b>0.20 <math>\pm</math> 0.13</b>	<b>2.84 <math>\pm</math> 2.55</b>	<b>0.10 <math>\pm</math> 0.09</b>	<b>0.31 <math>\pm</math> 0.17</b>

769

770 **Table 3.** Pigment:TChl *a* ratios for each algal group under low (SCM samples) and high  
771 (surface samples) **light** levels. (A) Initial ratio matrix determined from 1: This study; 2:  
772 Vidussi et al. (2004); 3: Higgins et al. (2011), (B) Final ratio matrix obtained after  
773 CHEMTAX recalculation in order to find the best fit between the *in situ* pigment  
774 concentrations and our initial ratio matrix. The symbol ‘-’ indicates similar ratios between  
775 low and high light levels. Pigment abbreviations are defined in Table 1. According to Higgins  
776 et al. (2011): Chryso-Pelago: Chrysophytes and Pelagophytes; Hapto-7: haptophytes type 7;  
777 Prasino-3: prasinophytes type 3; Prasino-2: prasinophytes type 2.  
778

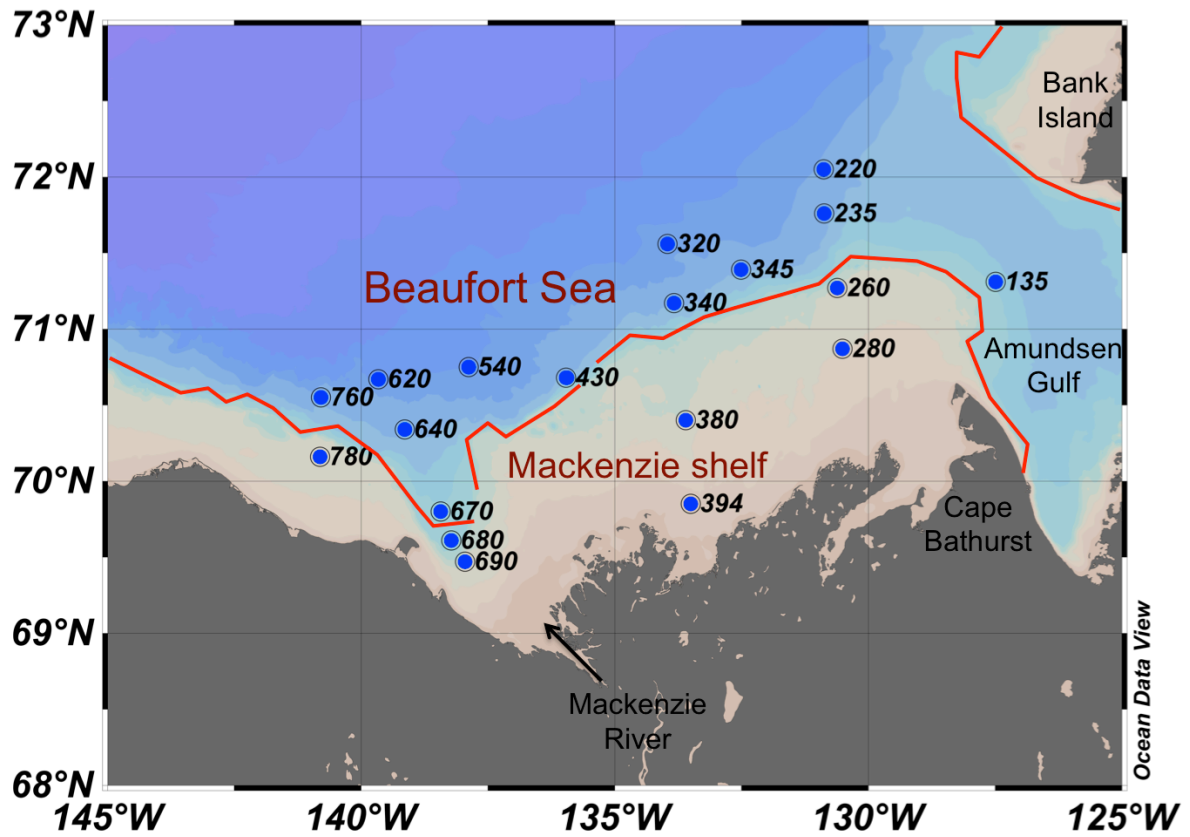
Class / Pigment	Light	Chl <i>c</i> <sub>3</sub>	Chl <i>c</i> <sub>1+2</sub>	But-fuco	Fuco	Hex-fuco	Neo	Pras	Chl <i>b</i>	Allo	Lut	Peri
<b>(A) Initial ratio matrix</b>												
<sup>1</sup> Diatoms	Low	0	0.171	0	0.425	0	0	0	0	0	0	0
	High	0	0.192	0	0.495	0	0	0	0	0	0	0
<sup>2</sup> Dinoflagellate	Low	0	0	0	0	0	0	0	0	0	0	0.6
	High	0	0	0	0	0	0	0	0	0	0	0.6
<sup>3</sup> <i>c</i> <sub>3</sub> -flagellates	Low	0.262	0.144	0.07	0.226	0.101	0	0	0	0	0	0
	High	0.179	0.126	0.081	0.3	0.194	0	0	0	0	0	0
<sup>3</sup> Cryptophytes	Low	0	0.104	0	0	0	0	0	0	0.277	0	0
	High	0	0.104	0	0	0	0	0	0	0.211	0	0
<sup>2</sup> Chryso-Pelago	Low	0.114	0.285	0.831	0.337	0	0	0	0	0	0	0
	High	0.114	0.316	1.165	0.425	0	0	0	0	0	0	0
<sup>3</sup> Hapto-7	Low	0.171	0.276	0.013	0.259	0.491	0	0	0	0	0	0
	High	0.215	0.236	0.023	0.42	0.682	0	0	0	0	0	0
<sup>3</sup> Prasino-2	Low	0	0	0	0	0	0.033	0	0.812	0	0.096	0
	High	0	0	0	0	0	0.056	0	0.786	0	0.038	0
<sup>3</sup> Prasino-3	Low	0	0	0	0	0	0.078	0.248	0.764	0	0.009	0
	High	0	0	0	0	0	0.116	0.241	0.953	0	0.008	0
<sup>3</sup> Chlorophytes	Low	0	0	0	0	0	0.036	0	0.339	0	0.187	0
	High	0	0	0	0	0	0.029	0	0.328	0	0.129	0
<b>(B) Final ratio matrix</b>												
<sup>1</sup> Diatoms	Low	0	0.091	0	0.301	0	0	0	0	0	0	0
	High	0	0.13	0	0.352	0	0	0	0	0	0	0
<sup>2</sup> Dinoflagellate	Low	0	0	0	0	0	0	0	0	0	0	0.375
	High	0	0	0	0	0	0	0	0	0	0	0.285
<sup>3</sup> <i>c</i> <sub>3</sub> -flagellates	Low	0.133	0.072	0.046	0.171	0.11	0	0	0	0	0	0
	High	0.145	0.08	0.039	0.125	0.056	0	0	0	0	0	0
<sup>3</sup> Cryptophytes	Low	0	0.079	0	0	0	0	0	0	0.162	0	0
	High	0	0.075	0	0	0	0	0	0	0.201	0	0
<sup>2</sup> Chryso-Pelago	Low	0.038	0.105	0.386	0.141	0	0	0	0	0	0	0
	High	0.044	0.111	0.324	0.131	0	0	0	0	0	0	0
<sup>3</sup> Hapto-7	Low	0.079	0.071	0.008	0.154	0.321	0	0	0	0	0	0
	High	0.036	0.061	0.006	0.122	0.303	0	0	0	0	0	0
<sup>3</sup> Prasino-2	Low	0	0	0	0	0	0.03	0	0.424	0	0.02	0
	High	0	0	0	0	0	0.017	0	0.418	0	0.049	0
<sup>3</sup> Prasino-3	Low	0	0	0	0	0	0.054	0.209	0.271	0	0.004	0
	High	0	0	0	0	0	0.043	0.136	0.222	0	0.005	0
<sup>3</sup> Chlorophytes	Low	0	0	0	0	0	0.035	0	0.037	0	0.143	0
	High	0	0	0	0	0	0.023	0	0.217	0	0.12	0

779

780 **Table 4.** Physical, chemical and biological characteristics (**mean  $\pm$  standard deviation**) for  
 781 each cluster presented in Fig. 4. **Cluster 1** is subdivided for samples collected in surface water  
 782 (surf) and sub-surface chlorophyll maximum (SCM) depth. PAR: Percentage of the surface  
 783 photosynthetically active radiation; C/TChl *a*: ratio of algal carbon biomass to total  
 784 chlorophyll *a* concentration (i.e. TChl *a* = Chl *a* + Chl *d* *a*).  
 785

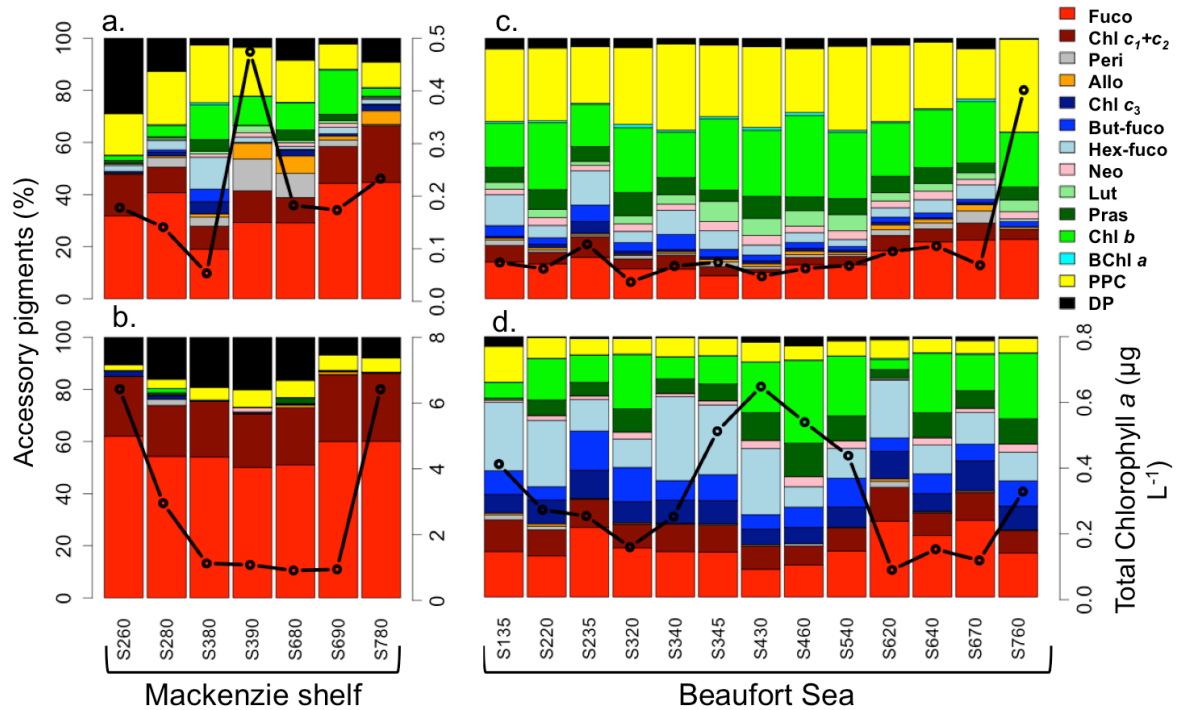
	Depth (m)	T (°C)	Salinity	PAR ( $\mu\text{M m}^{-2} \text{s}^{-1}$ )	NO <sub>3</sub> <sup>-</sup> ( $\mu\text{mol L}^{-1}$ )	NH <sub>4</sub> <sup>+</sup> ( $\mu\text{mol L}^{-1}$ )	PO <sub>4</sub> <sup>3-</sup> ( $\mu\text{mol L}^{-1}$ )	TChl <i>a</i> ( $\mu\text{g L}^{-1}$ )	C/TChl <i>a</i>
<b>Cluster 1 (n=11)</b>	24 $\pm$ 16	0.8 $\pm$ 2.7	30.2 $\pm$ 3.0	39 $\pm$ 78	3.1 $\pm$ 2.8	0.09 $\pm$ 0.11	0.96 $\pm$ 0.41	1.80 $\pm$ 2.35	140 $\pm$ 150
<i>Cluster 1 surf (n=4)</i>	5 $\pm$ 3	4.2 $\pm$ 1.1	26.7 $\pm$ 3.7	100 $\pm$ 110	0.2 $\pm$ 0.2	0.01 $\pm$ 0.01	0.50 $\pm$ 0.14	0.16 $\pm$ 0.04	280 $\pm$ 150
<i>Cluster 1 SCM (n=7)</i>	35 $\pm$ 8	-1.0 $\pm$ 0.1	31.7 $\pm$ 0.4	2.2 $\pm$ 2.3	5.1 $\pm$ 1.6	0.15 $\pm$ 0.12	1.27 $\pm$ 0.11	2.73 $\pm$ 2.55	49 $\pm$ 23
<b>Cluster 2 (n=15)</b>	2 $\pm$ 1	3.7 $\pm$ 2.9	24.1 $\pm$ 6.4	129 $\pm$ 85	0.1 $\pm$ 0.1	0.02 $\pm$ 0.04	0.54 $\pm$ 0.10	0.12 $\pm$ 0.13	160 $\pm$ 110
<b>Cluster 3 (n=8)</b>	66 $\pm$ 4	-1.1 $\pm$ 0.1	31.5 $\pm$ 0.2	2.2 $\pm$ 1.2	5.1 $\pm$ 2.7	0.02 $\pm$ 0.02	1.26 $\pm$ 0.20	0.28 $\pm$ 0.16	38 $\pm$ 23
<b>Cluster 4 (n=6)</b>	56 $\pm$ 5	-1.1 $\pm$ 0.1	31.0 $\pm$ 0.4	4.7 $\pm$ 1.7	0.5 $\pm$ 0.2	0.03 $\pm$ 0.02	0.86 $\pm$ 0.06	0.36 $\pm$ 0.20	34 $\pm$ 25

786



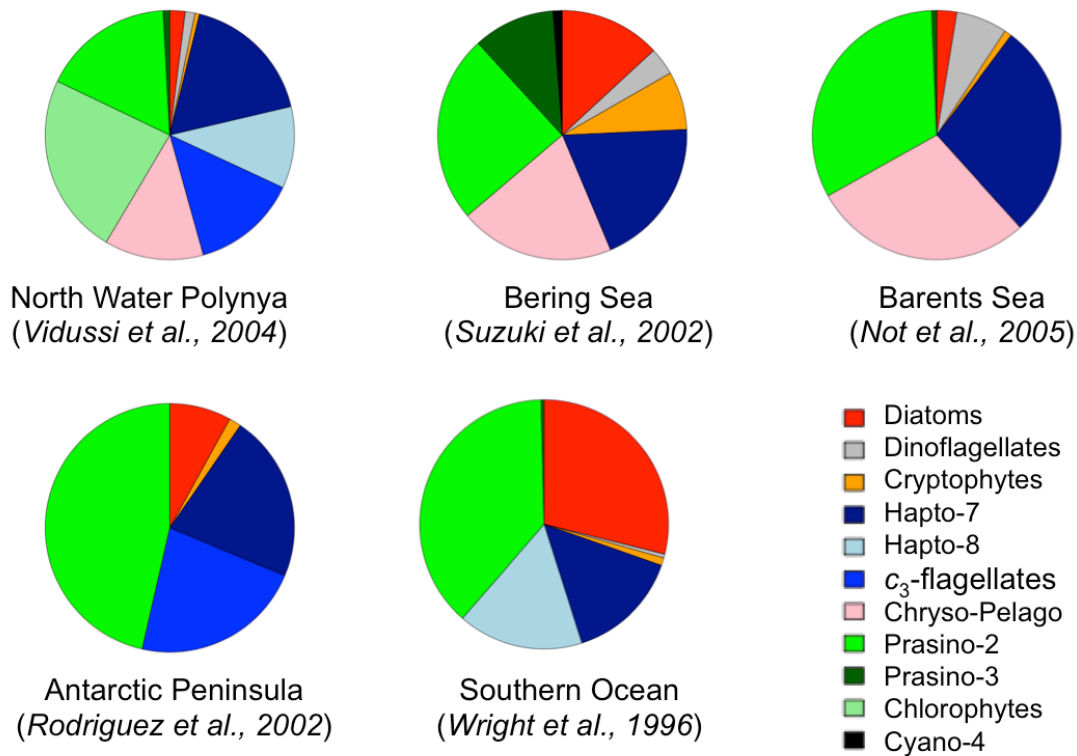
787  
788  
789  
790  
791

**Figure 1.** Location of the sampling stations in the Canadian Beaufort Sea from 30 July to 27 August 2009 during the MALINA expedition. The isobath 150 m (in red) separates the Mackenzie shelf from the deep waters of the Beaufort Sea.



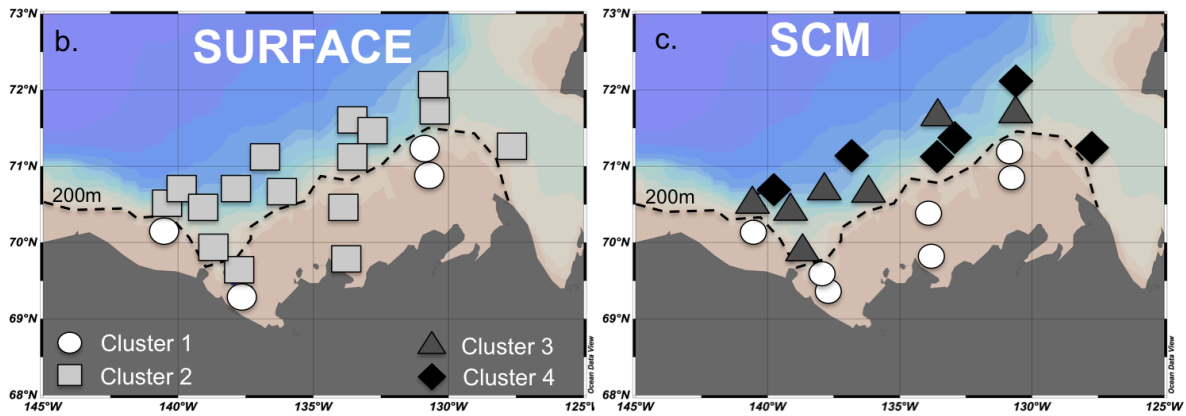
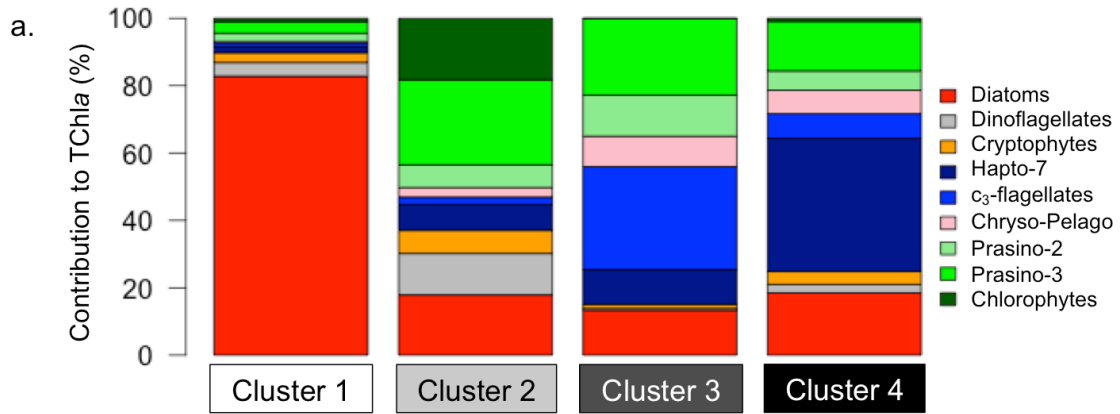
792  
 793  
 794  
 795  
 796  
 797  
 798  
 799  
 800  
 801

**Figure 2.** Relative contribution of accessory pigments to total accessory pigment (wt:wt) in (a, c) surface water and at the (b, d) sub-surface chlorophyll maximum (SCM) depth of the (a, b) Mackenzie shelf and (c, d) deep waters of the Beaufort Sea. The black line with circle represents the chlorophyll *a* concentration. DP: degradation pigments (Chlide *a* + Pheide *a* + Phe *a*); PPC: photoprotective carotenoids (i.e. Diadino + Diato + Zea + Viola + Car). Pigment abbreviations are defined in Table 1. Please note the different TChl*a* scales between the four panels. The same TChl*a* scale (0 to 0.8  $\mu\text{g L}^{-1}$ ) was used for the panels c and d.



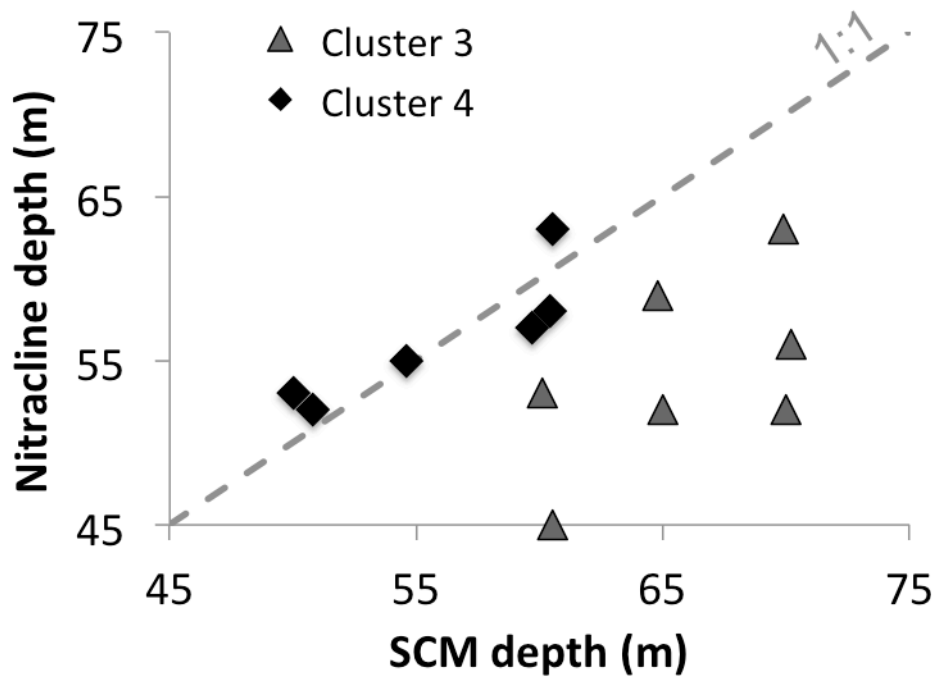
802  
803  
804  
805  
806  
807  
808  
809  
810  
811  
812  
813

**Figure 3.** Average contribution of major algal groups to total chlorophyll *a* (Chl *a*) concentration at the sub-surface chlorophyll maximum (SCM) depth in the deep waters of the Beaufort Sea calculated with the CHEMTAX software using five different pigment/Chl *a* ratio matrices. Ratio matrices are from previous studies conducted in polar oceans: Vidussi et al. (2004) in North Water Polynya, Suzuki et al. (2002) in Bering Sea, Not et al. (2005) in Barents Sea, Rodriguez et al. (2002) in Antarctic Peninsula and Wright et al. (1996) in Southern Ocean. According to Higgins et al. (2011): Hapto-7: haptophytes type 7; Hapto-8: haptophytes type 8; Chryso-Pelago: Chrysophytes and Pelagophytes; Prasino-2: prasinophytes type 2; Prasino-3: prasinophytes type 3; Cyano-4: cyanobacteria type 4.



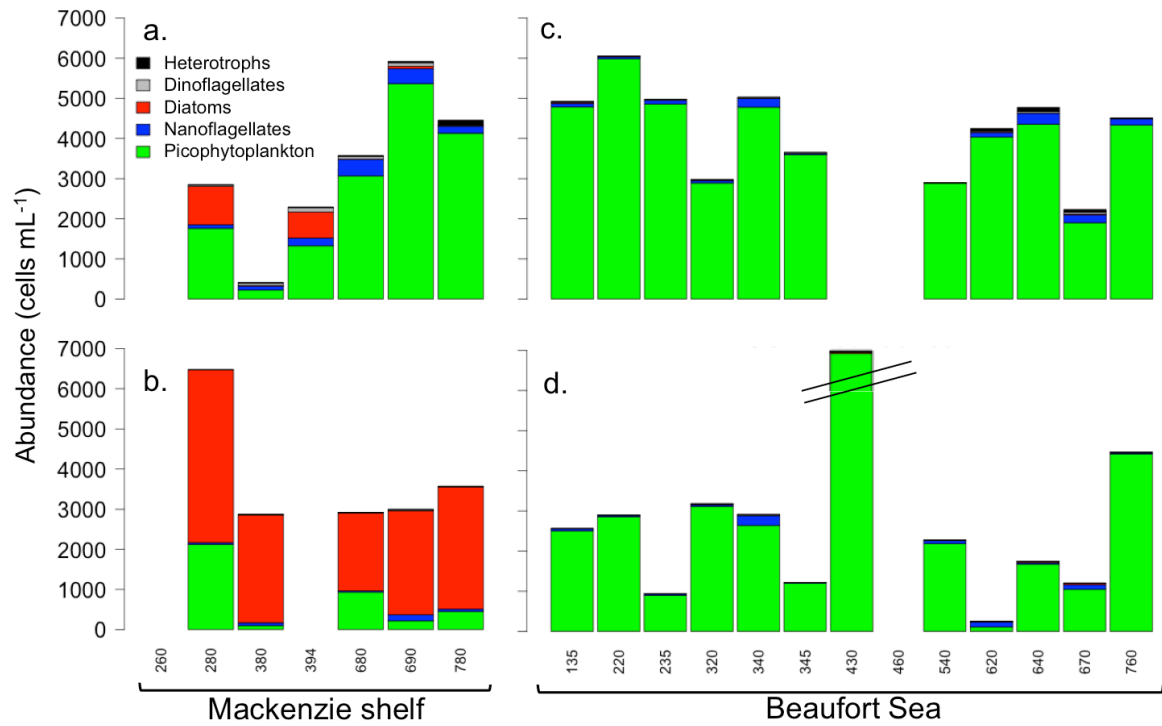
814  
815  
816  
817  
818  
819  
820  
821  
822

**Figure 4.** (a) Relative contribution of major algal groups to total chlorophyll *a* (Chl *a*) concentration (calculated by CHEMTAX) for four groups of samples with similar pigment composition (clusters) determined with the k-means clustering method (MacQueen, 1967). The geographical position of the four groups of samples (4 clusters) is mapped for the (b) surface water and (c) sub-surface chlorophyll maximum (SCM) depth. According to Higgins et al. (2011): Hapto-7: haptophytes type 7; Chryso-Pelago: Chrysophytes and Pelagophytes; Prasino-2: prasinophytes type 2; Prasino-3: prasinophytes type 3.

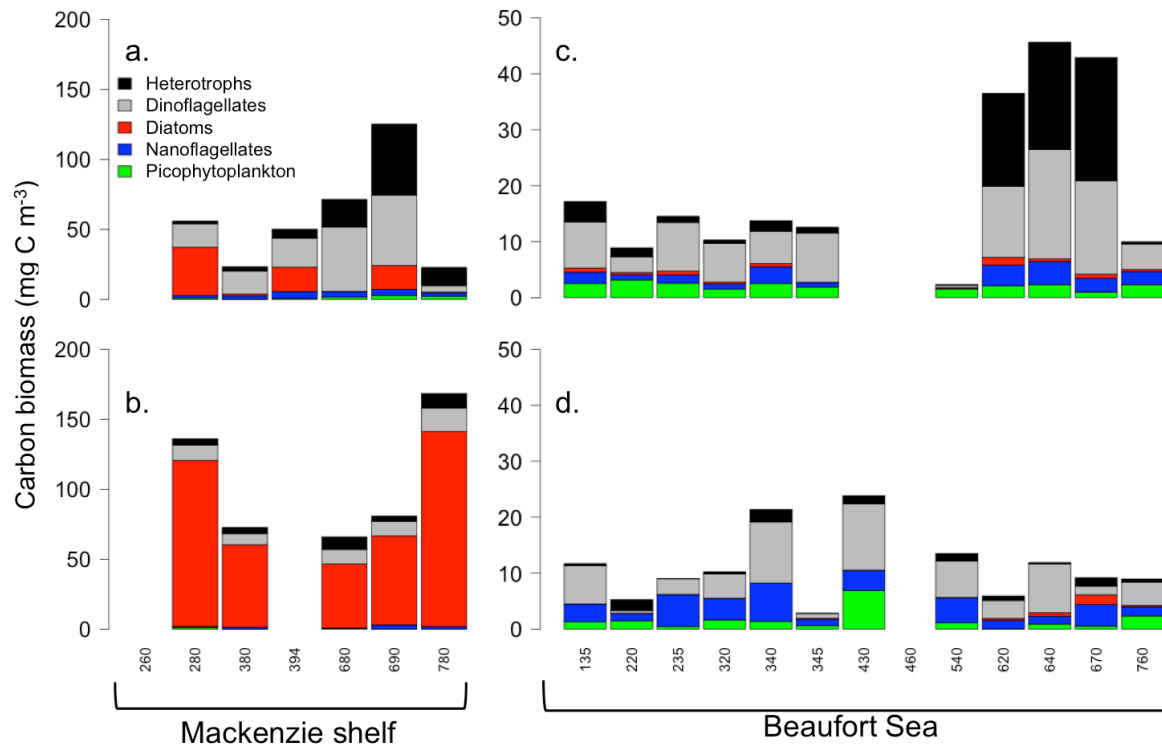


823  
 824  
 825  
 826  
 827  
 828  
 829  
 830

**Figure 5.** Relationship between the nitracline depth and the sub-surface chlorophyll *a* maximum (SCM) depth for samples of clusters 3 (grey triangle) and 4 (black diamond). The dashed line represents a 1:1 relationship. Note the SCM depth matches with the nitracline depth for cluster 4 samples. In contrast, the SCM is deeper than the nitracline depth for cluster 3 samples.

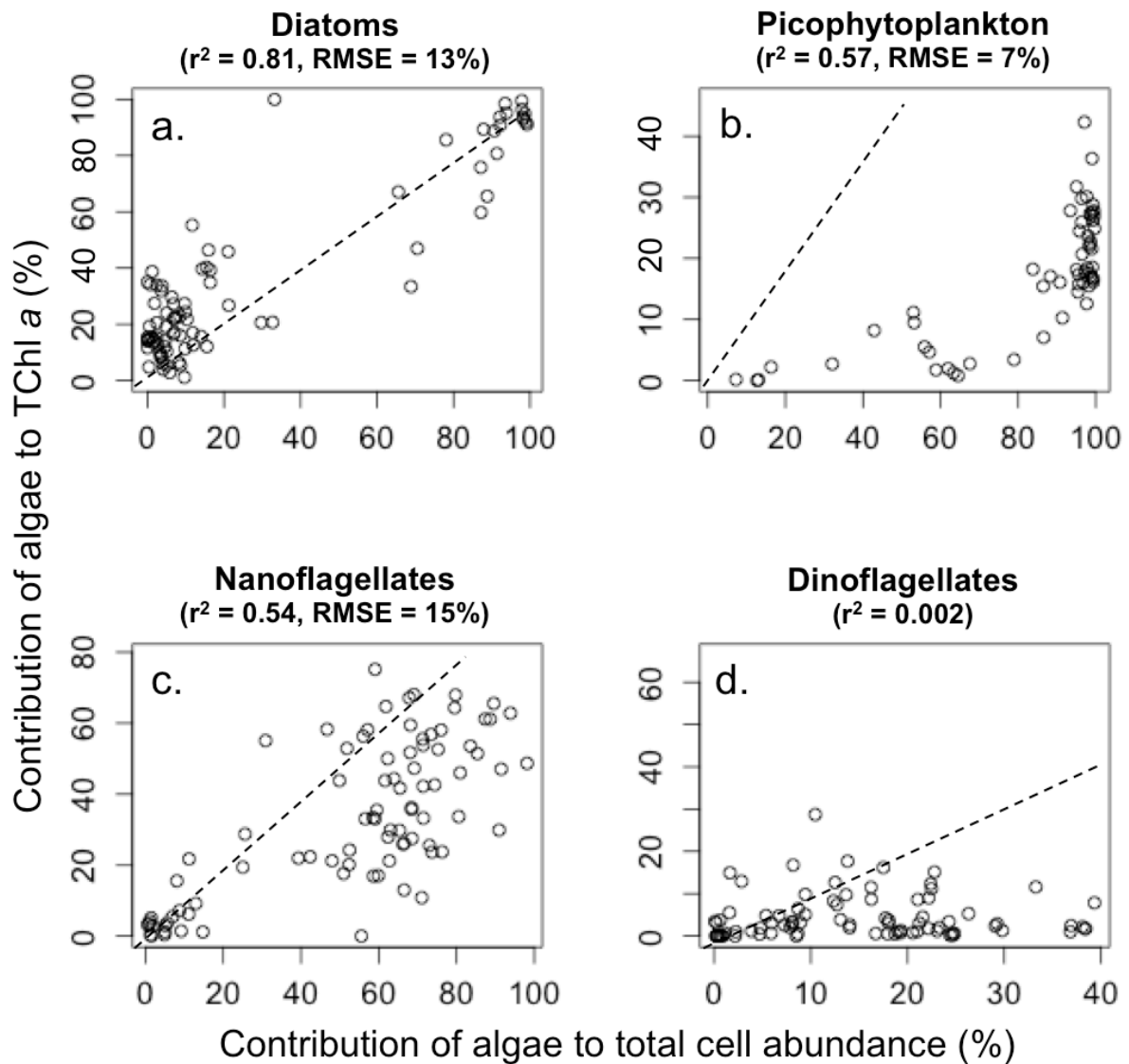


831  
 832 **Figure 6.** Abundance of five protist groups in (a, c) surface and at the (b, d) subsurface  
 833 chlorophyll maximum (SCM) depth of the (a, b) Mackenzie shelf and (c, d) deep waters of the  
 834 Beaufort Sea.  
 835



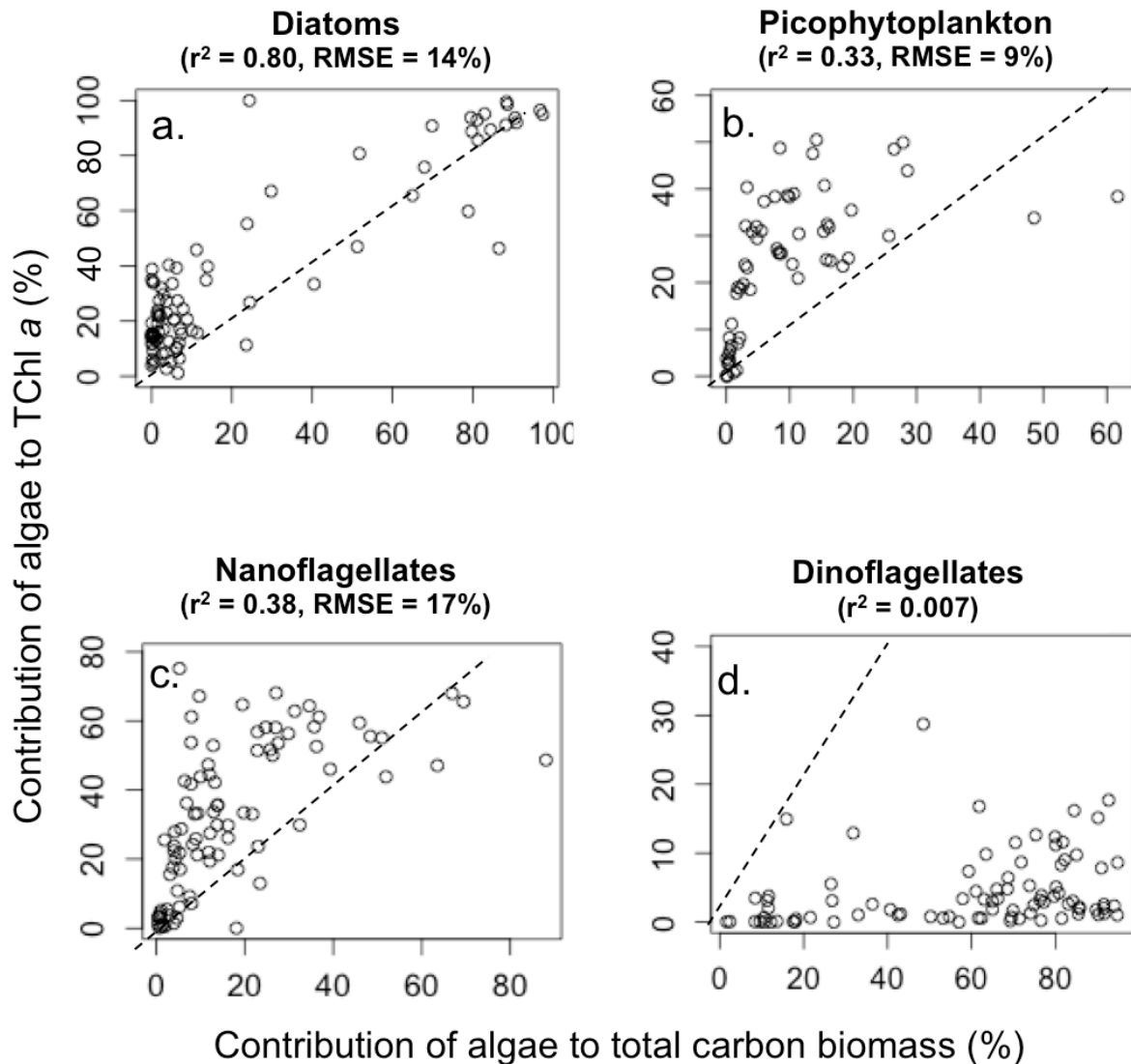
836  
837  
838  
839  
840

**Figure 7.** Carbon biomass of five protist groups in (a, c) surface and at the (b, d) subsurface chlorophyll maximum (SCM) depth of the (a, b) Mackenzie shelf and (c, d) deep waters of the Beaufort Sea.



841  
 842  
 843  
 844  
 845  
 846  
 847  
 848  
 849  
 850  
 851

**Figure 8.** Scatter diagrams of the contribution of (a) diatoms, (b) picophytoplankton, (c) nanoflagellates and (d) dinoflagellates to total chlorophyll *a* (Chl *a*) concentration (calculated by CHEMTAX) as a function of their contribution to total cell abundance. The dashed line represents the 1:1 relationship. The Pearson correlation coefficient ( $r^2$ ) is indicated for each algal group. The root mean square error (RMSE) depicts the predictive capabilities of cell abundance from the CHEMTAX-derived algal groups. 95% of the algal cell abundance estimated from the CHEMTAX-derived algal groups are in the range  $\pm 2 \times \text{RMSE}$  from the least square regression line.



852  
853  
854  
855  
856  
857  
858  
859  
860  
861  
862

**Figure 9.** Scatter diagrams of the contribution of (a) diatoms, (b) picophytoplankton, (c) nanoflagellates and (d) dinoflagellates to total chlorophyll *a* (Chl *a*) concentration (calculated by CHEMTAX) as a function of their contribution to total carbon biomass (calculated from biovolume, see Materials and methods). The dashed line represents the 1:1 relationship. The Pearson correlation coefficient ( $r^2$ ) is indicated for each algal group. The root mean square error (RMSE) depicts the predictive capabilities of carbon biomass from the CHEMTAX-derived algal groups. 95% of the algal carbon biomass estimated from the CHEMTAX-derived algal groups are in the range  $\pm 2 \times \text{RMSE}$  from the least square regression line.